

Article

BATS: Adaptive Ultra Low Power Sensor Network for Animal Tracking

Niklas Duda^{1,*} , Thorsten Nowak², Markus Hartmann², Michael Schadhauer², Björn Cassens³, Peter Wägemann⁴, Muhammad Nabeel⁵, Simon Ripperger^{6,7}, Sebastian Herbst⁸, Klaus Meyer-Wegener⁸, Frieder Mayer^{6,9}, Falko Dressler⁵, Wolfgang Schröder-Preikschat⁴, Rüdiger Kapitza³, Jörg Robert² , Jörn Thielecke², Robert Weigel¹  and Alexander Kölpin¹⁰ 

¹ Institute for Electronics Engineering, Friedrich-Alexander University of Erlangen-Nürnberg;

² Institute of Information Technology, Friedrich-Alexander University of Erlangen-Nürnberg;

³ Institute of Operating Systems and Computer Networks, TU Braunschweig;

⁴ Chair of Computer Science 4 – Distributed Systems and Operating Systems, Friedrich-Alexander University of Erlangen-Nürnberg;

⁵ Heinz Nixdorf Institute and Dept. of Computer Science, Paderborn University;

⁶ Museum für Naturkunde, Leibniz-Institute for Evolution and Biodiversity Science;

⁷ Smithsonian Tropical Research Institute;

⁸ Chair of Computer Science 6 – Data Management, Friedrich-Alexander University of Erlangen-Nürnberg;

⁹ Berlin-Brandenburg Institute of Advanced Biodiversity Research (BBIB);

¹⁰ Chair for Electronics and Sensor Systems, Brandenburg University of Technology;

* Correspondence: niklas.duda@fau.de; Tel.: +49 (0)9131-85-25023

Version September 25, 2018 submitted to *Sensors*

Abstract: In this paper, the BATS project is presented which aims to track the behavior of bats via an ultra-low power wireless sensor network. An overview about the whole project and its parts like sensor node design, tracking grid and software infrastructure is given and the evaluation of the project is shown. The BATS project includes a lightweight sensor node that is attached to bats and combines multiple features. Communication among sensor nodes allows tracking of bat encounters. Flight trajectories of individual tagged bats can be recorded at high spatial and temporal resolution by a ground node grid. To increase the communication range the BATS project implemented a long-range telemetry system to still receive sensor data outside the standard ground node network. The whole system is designed with the common goal of ultra-low energy consumption while still maintaining optimal measurement results. To this end, the system is designed in a flexible way and is able to adapt its functionality according to the current situation. In this way it uses the energy available on the sensor node as efficient as possible.

Keywords: wireless sensor networks; animal tracking; adaptive sensor network

1. Introduction

Biologging or the remote tracking of animals by means of attached tags is motivating interdisciplinary research for more than 50 years and has been strongly technology-driven ever since. While biologists have mainly focused on individual movement patterns during the first decades of biologging research, applications have become much broader recently by the availability of digital transceivers and manifold sensors for designing animal borne tags. Advances in biologging technology have motivated innovative research in the fields of movement ecology, sociobiology or conservation biology, which relies on detailed information on the behavior of individual animals [1–3]. For example, biologging studies have revealed how movement rates of mammals respond to anthropogenic impact [4] or how social groups of primates make decision on where to move [5].

24 Advanced biologging devices such as GPS-tags automatically collect data and enable remote
25 download, which allows for the observation of large numbers of individuals at a time, maximizes data
26 recovery rates and minimizes the impact on study objects. Generated datasets become increasingly
27 rich since integrated sensors collect precise information on physiological or environmental conditions
28 in addition to the location of the tagged animals. However, researchers always face the trade-off
29 between performance and device weight since more complex functionalities come at the cost of
30 higher energy expense which translates into higher tag weight by the demand for a bigger battery.
31 Energy harvesting solutions, such as solar cells, recharge the battery while the animal is on the move
32 and extend battery life. However, applications are mainly restricted to diurnal taxa which range
33 in sun-exposed environments and its recharging efficiency may depend upon weather or seasonal
34 conditions [6]. In turn, tag weight dictates the spectrum of animal species which can be studied
35 because tags constitute a burden to the animal, which may induce unintended changes in behavior or
36 even reduce fitness or survival rates [7]. Considerations for tag to body weight ratio vary across taxa
37 suggesting tags not to exceed 3-5% or for short-term studies a maximum of 10% of the body weight
38 [8–11]. Due to these limitations and the considerably large size and weight of most fully automated
39 tracking devices, around two thirds of avian and mammalian species still cannot be studied [2]. For
40 this reason older techniques which originated between the 60s and 90s of the last century, which rely
41 on smaller but less powerful animal-borne devices such as VHF-transmitters, geolocators or PIT tags
42 still represent the state-of-the-art for studying smaller vertebrates like songbirds, rodents or bats.

43 The most diverse part of the mammalian and avian range of species is at a body mass of
44 around 10-20 g [2] and can therefore only be studied with tags that weigh 2 g or less. Hence, the
45 further miniaturization of biologging technologies, which are capable of fully automated tracking
46 of miniaturized tags at high spatial and temporal resolution, collecting complementary sensor data
47 and remote access for download and reconfiguration would represent a quantum-leap for biologging
48 research. Wireless sensor networks (WSNs) may be an ideal solution to meet the aforementioned criteria
49 if hardware, software and communication protocols are designed with the goal of ultra-low-power
50 consumption in order to ensure an acceptable runtime of at least 1-2 weeks. We present an adaptive
51 and reconfigurable ultra-low-power WSN for biologging which enables ground-based localization at
52 high temporal and spatial resolution, communication among animal-borne tags for direct encounter
53 detection and remote data access, optionally via long-range telemetry. We verify our developments
54 by tracking free-ranging bats, an animal group which is particularly difficult to observe due to its
55 nocturnal activity, high mobility and small body weight of most species.

56 2. Related Work

57 Most available advanced animal tracking systems rely on relatively big mobile nodes. These
58 of course comprise broader functionality, however, they cannot be used for tracking small-bodied
59 animals like most bat species. Here the strict size and weight constraints limit the scope of suitable
60 tracking methods. In the past a common approach was to use VHF-Tags which periodically send a
61 modulated signal that can be used to track the animal. Due to the nature of these tags it requires a
62 lot of manual work to track the animals and the number of track-able individuals at the same time
63 is limited. Also these tags do not provide any additional information about the individual besides a
64 rough geographic position.

65 In the following some advanced systems that allow automated tracking of multiple individuals
66 and are focusing on small-bodied species are shortly described.

67 2.1. Ground based tracking

68 The **ATLAS** [12] system ('Advanced Tracking and Localization of Animals in real-life Systems')
69 bases on a time-of-arrival principle for reliable localization of digital transceivers, which weigh around
70 1 g, over distances of up to 15km. The initial real-world deployment of the ATLAS system consisted of
71 9 base stations covering an area of several km² in the Hula Valley in Israel. The runtime of the nodes is

72 highly weight depended. A 1.5 g heavy tag can reach a runtime of 10 days. A 10 g heavy node already
73 reached a runtime of 100 days. The system can track the transceivers with a standard deviation of 5 m,
74 which is comparable in terms of accuracy to GPS-tracking devices and allows studying space use at a
75 high spatial resolution.

76 The **MOTUS** wildlife tracking system [13] benefits from the light weight of traditional VHF tags
77 by tracking animals over large geographic scales in a collaborative approach. Arrays of automated
78 receivers, which are curated by different research groups, detect digital radio-telemetry transmitters
79 emitting signals at a single frequency. This way all participants obtain data from collaboratively
80 maintained infrastructure. The VHF-tags used in the MOTUS project, which are relatively simple in
81 terms of functionality, weigh 0.2 to 2.6 g at lifetimes of 10 days to 3 years. The tags send out an unique
82 signal, respectively, and that way an unique ID can be assigned to each tag. The system supports up to
83 500 unique IDs. The reception range of the used base stations is between 500 m to 15 km depending on
84 the antenna setup. The location of the tag gets derived from which station receives the signal. So while
85 the system covers a large geographic scale the resolution in this area is limited, making the setup an
86 ideal instrument for tracking large-scale movement of animals.

87 **Encounternet** [14] is an approach for automated encounter logging to study social behavior in
88 wild animals. Other than previous encounter tracking implementations it does not require retrieving
89 the sensor nodes but includes ground stations which are downloading the recorded data from the
90 mobile nodes. The Encounternet tags have a runtime of about 7.5 days when used only as transmitters
91 and 21 hours in real proximity logging mode with transmitting and receiving enabled while having
92 a weight of 1.3 g. This allows the encounter tracking of lightweight species but has highly limited
93 runtime and does not include absolute location tracking. Previous versions of the Encounternet sensor
94 nodes still had a weight of 10 g and have been used for proximity logging over a time period of ca.
95 2 months in a single deployment [15].

96 2.2. *Satellite based tracking*

97 Traditional **GPS trackers** are widely used for animal tracking. These contain a GPS module which
98 is periodically woken up to perform a GPS fix to record its location. Depending on the system it
99 is required to recover the tags to download the recorded fixes from the internal memory or the tag
100 contains a mobile network modem to automatically upload the data. The smallest versions of simple
101 loggers can be as light as 1 g, but they can only record around 100 fixes over several days. If long-term
102 high-resolution tracking and an option for remote download are required, tag weight rapidly increases
103 [2]. While these tracker reach high spatial resolution in free space (like tracking migrating birds while
104 flying), data quality may suffer when animals are located in places with poor GPS reception such as
105 thick forests or inside roosts (e.g. cavern or tree holes).

106 The **ICARUS** project [16] ('International Cooperation for animal Research Using Space') has
107 the goal to enable tracking of small objects such as migratory bats or birds. This is achieved via an
108 antenna attached to the International Space Station (ISS), which receives data from animal-borne
109 tags. The mobile tags document their location via GPS and contain accelerometer, magnetometer and
110 temperature sensors. Whenever the ISS is in range the recorded positions and sensor data will be
111 uploaded to the ISS and from there stored in a database. The big advantage of the ICARUS project is
112 the relatively low orbit of the ISS. Thus uploading of data can be realized even with low energy and
113 therefore tags can be smaller than conventional GPS trackers with remote access. The ISS uplink of the
114 ICARUS project allows nearly global coverage. The current state of the project uses sensor tags with a
115 weight of 5 g and volume of 2 cm². Thanks to supporting solar cells, the runtime can be extended over
116 the one supported by the battery capacity as long as diurnal species are investigated. There are plans
117 to further reduce the weight of the sensor nodes by reducing the functionality to support tracking of
118 even smaller animals.

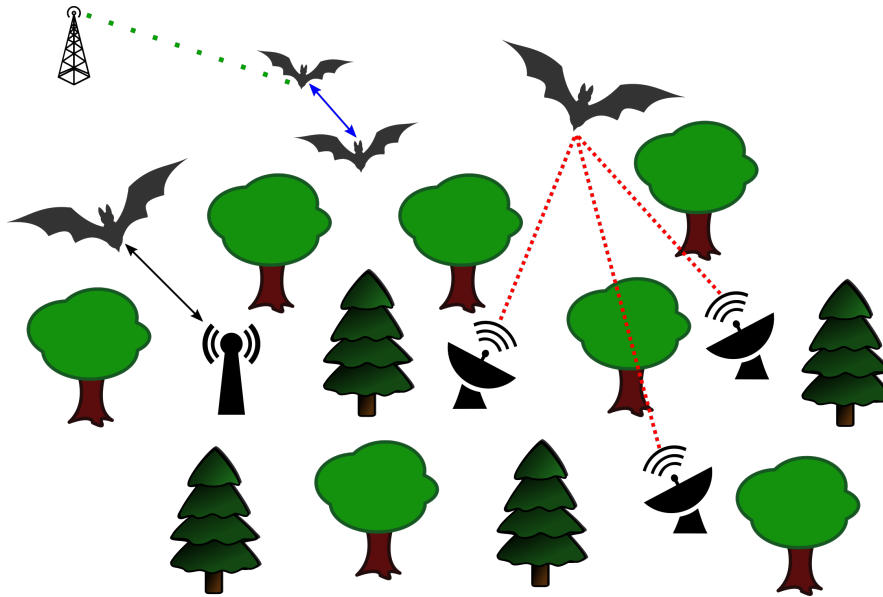


Figure 1. Conceptual overview about the abilities of the BATS system: Trajectory tracking (red dotted line), Encounter Detection (node to node communication in solid blue and download in solid black) and Long Range Telemetry (dotted green)

119 3. BATS System overview

120 The BATS Project¹ aims to solve the challenges described in Section 1. The project is split into
 121 multiple sub-projects, each working on specific details of the whole system. An overview of the
 122 application of the BATS project is given in Fig. 1. The system allows a so called encounter detection,
 123 meaning that the sensor tags can notice that another tagged bat is close and record the duration of the
 124 meeting as well as estimate a rough distance based on RSSI values (blue solid line). The encounter
 125 detection works independent of any ground station network and can record the encounter data till a
 126 base station is in range again and downloads the data (black solid line). While being in the ground
 127 station tracking network, in addition to simple encounter detection, the BATS system also allows the
 128 localization of the bats in reference to the ground network and the recording of flight trajectory. This
 129 is achieved by calculating an expected position of the bat based on the signal received by multiple
 130 base stations (red tightly dotted line). To be less dependent on the bat staying in the ground network,
 131 we also implemented a long range telemetry system that can receive data of the bats over a high
 132 range (green light dotted line). The long range however results in a limited data rate. This makes it
 133 impossible to transmit the same data as in the ground node network but still we are able to get some
 134 information about the investigated individuals.

135 The implementation of all functions of the BATS project focuses on minimizing the energy
 136 consumption of the mobile node. Systems for node to node communication like Bluetooth 5 [17]
 137 and long range telemetry like LoRa are already available. However, using them is not feasible here
 138 since it would require to implement multiple protocols with their corresponding overhead in order
 139 to realize the complete set of functionalities of the BATS system. Even though Bluetooth 5 allows
 140 efficient energy management for wireless sensor networks [18], we would not consider Bluetooth
 141 or other already existing systems a suitable solution for node to node communication in the BATS
 142 project since the research object "bat" poses a set of new challenges compared to industrial sensor
 143 networks. This is mostly due to the behavior and habitat of bats as well as the strict weight and

¹ <http://www.for-bats.org/>

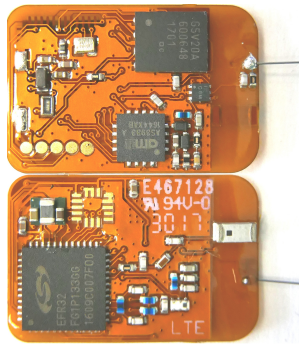


Figure 2. Front and back of mobile node

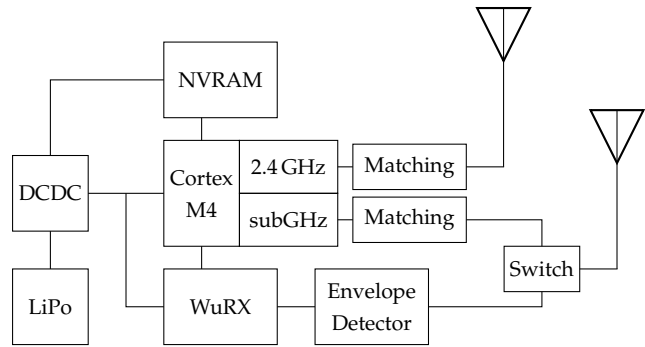


Figure 3. Overview of mobile node design

144 size limit. By implementing our own radio protocols we can keep the overhead low and allow fast
 145 switching between the different operating modes.

146 The following chapters will give an insight about how the single parts of the BATS system are
 147 build. The mobile sensor node with the embedded software is the central part of the sensor network
 148 and gets attached to the bats. Depending on the desired application mode and the location of the bat
 149 a different set of ground network nodes communicates with the sensor tag on the bat for encounter
 150 detection data download, localization or long range telemetry. As final step we developed methods
 151 to sort the vast amount of collected data to allow researches to investigate the biologic questions this
 152 system was developed to answer.

153 3.1. Mobile Node

154 3.1.1. Overall Functionality

155 For the monitoring the activity of bats, these have to be tagged with a wireless sensor node. The
 156 current version of the BATS sensor node is shown in Figure 2. Attached to the bat the mobile node
 157 serves multiple functions which are depending on the current location of the bat. We introduced so
 158 called zones that change the actual behavior of the tag. If in range of the ground tracking grid (chapter
 159 3.3), two beacons are sent out at 868/915 MHz and 2.4 GHz 8 times per second. Otherwise these
 160 beacons are omitted to save energy. The current zone respectively operating mode is set by beacons
 161 sent from a ground station. In the current implementation the encounter detection is active regardless
 162 of the current location and beacons are periodically sent out for other mobile nodes to receive.

163 3.1.2. Hardware Setup

164 An overview about the architecture of the BATS mobile node is shown in Fig. 3. A Silabs EFR32
 165 Flex Gecko System-on-Chip (SoC) is the central component in the design. It combines a Cortex M4
 166 processor core with two radio frontends, one for the 2.4 GHz ISM Band and one subGHz transceiver.
 167 Depending on the desired location for the sensor network the frequency of the subGHz transceiver is
 168 set to the 868 MHz (Europe) or 915 MHz (America) band. The wake-up functionality is implemented
 169 with an AMS AS3933 wake-up receiver put behind an envelope detector. The envelope detector is
 170 used to extract the low frequency wake-up pattern from the high frequency radio signal. To increase
 171 the data storage capacity a Ferroelectric Random Access Memory (FRAM) is used as Non-Volatile
 172 Random Access Memory (NVRAM). The advantages of FRAM compared to standard flash memory
 173 are the highly reduced power consumption and fast read and write access. A detailed description of
 174 the selected hardware can be found in [19].

175 The system can easily be expanded with additional functionality like new sensors. An
 176 accelerometer could be used for activity detection of bats and in combination with a magnetometer
 177 and gyroscope the inclination and heading direction could be calculated. However, the focus in the

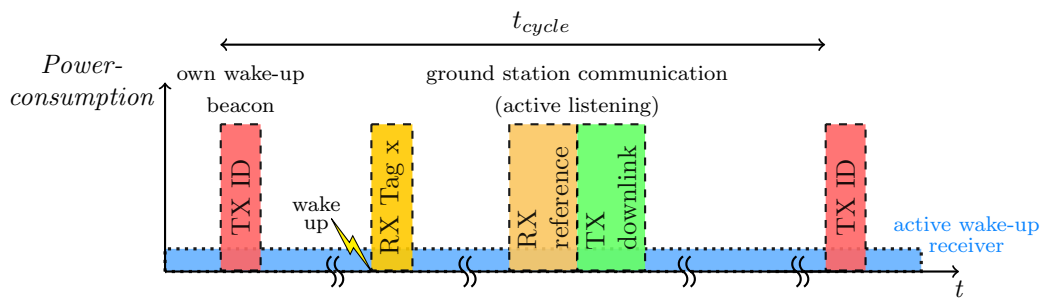


Figure 4. Wake-up receiver based communication scheme

178 proposed design was on a ultra light weight and ultra low power system. Thus, no additional sensors
 179 are used in the current version of the BATS mobile node.

180 3.1.3. Wake-Up Receiver Based Communication Approach

181 The key part of the proximity sensing is the node to node communication. Especially with a high
 182 number of supported nodes it is not feasible anymore to turn on the radio in predefined time slot to
 183 receive potential packages. Instead it would be necessary to constantly listen to incoming packages.
 184 To still be able to keep the power consumption to a minimum the BATS mobile node makes use of a
 185 wake-up receiver based approach. This ultra low power receiver is constantly in receiving mode and
 186 wakes up the remaining circuit upon reception of a special beacon. The downside of the low power
 187 consumption is the relatively low sensitivity of -43 dBm and thus a limited range of a few meters. For
 188 proximity logging however this is the preferred behavior. This way only close encounters will activate
 189 the system and it is not necessary to implement a software Received Signal Strength Indicator (RSSI)
 190 threshold. This way the amount of unnecessary wake-ups can be greatly reduced since bats that are
 191 more than 5 m away don't trigger wake-ups anymore. The 5 m range of the wake-up receiver has been
 192 evaluated during field tests (see chapter 4) in mature forest environment by measuring the distance
 193 between which the nodes still have reception.

194 The mobile node periodically sends out its own On-Off-Keying (OOK) modulated wake-up
 195 beacons composed of the wake-up pattern and payload data like the own node ID as seen in red
 196 as "TX ID" in Fig. 4 with a transceiver power of 10 dB. Upon receiving such beacon from another
 197 node the system wakes up (yellow lightning bolt), receives the remaining part of the beacon via the
 198 conventional receiver (orange) and triggers the data processing as described in section 3.2. If a false
 199 wake up would be triggered the following communication based on the conventional receiver would
 200 fail and no encounter is detected.

201 Since beacons are usually sent out every two seconds the channel has a relatively low utilization
 202 even if multiple bats are present. Channel utilization is further optimized by automated reduction of
 203 the beaconing frequency in the roost which is the location with the highest probability of encounters.
 204 Thus interference between nodes is not seen as a problem. If a packet collision should still occur, the
 205 beacon reception will fail and no encounter will be recorded. To increase the system robustness against
 206 package loss during meetings (due to beacon collision or other reasons) up to 5 beacons can get lost
 207 without interrupting the corresponding meeting. Depending on the current use case of the system
 208 these values (beaconing frequency depending on location as well as maximum beacon loss) can be
 209 adapted flexibly.

210 While for the proximity sensing the short reception range of the wake-up receiver is an advantage,
 211 the usually high distance between the base station and the bats prevents the wake-up receiver to detect
 212 signals from the base station. Thus, to be able to receive the base station data the node periodically
 213 turns on the conventional receiver to check for base stations in range. Other than the mobile nodes the
 214 base station doesn't have any strict energy constraints and the base stations are placed so that they

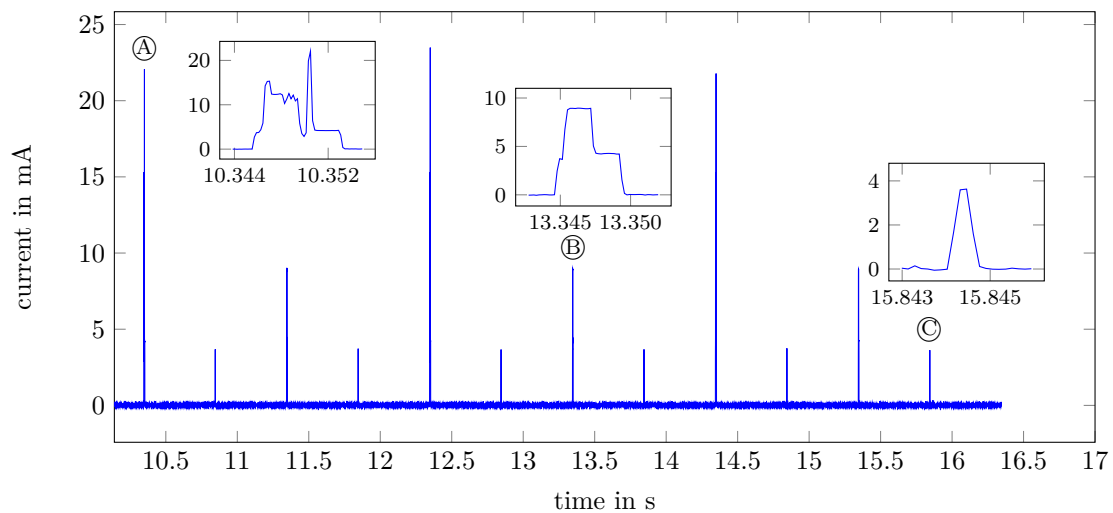


Figure 5. Measurement of the energy consumption of a BATS mobile node. The subplots next to the peaks marked **A**, **B**, **C** show the detailed current consumption during these peaks.

215 can't interfere with each other. This allows the base station to transmit during all available time slots.
 216 This way, the time the receiver is turned on doesn't have to be synchronized with the base station,
 217 allowing the receiver to be active only a short period of time. Even though a conventional receiver
 218 is being used here, this way the energy consumption can be kept at a minimum. If a base station in
 219 range has been detected (marked dark orange in Fig. 4) the *Base-Station Handler* described in section
 220 3.2 handles the communication.

221 3.1.4. Power Management

222 Despite the limited weight and battery capacity, the sensor node should be powered for as long as
 223 possible. A lithium polymer battery with 25 mAh and a weight of 0.66 g has been chosen as power
 224 supply. Apart from a relatively high capacity in regards to its weight and size, the battery supports a
 225 peak current of around 25 mA. This is necessary to be able to power the radio to transmit/receive data.
 226 Compared to the used lithium polymer battery, coin prime cells are available in even higher capacities
 227 while still fitting the weight constraints. However, they only allow a low current draw. Since the active
 228 time of the node depends on received wake-up packages the current consumption can not be predicted.
 229 Thus a buffer solution that would smoothen the current peaks to suitable low levels can't be used.

230 While the used NVRAM already has a much lower current consumption as comparable flash
 231 memory it still draws the highest current on the mobile node. To further decrease the current
 232 consumption the NVRAM can be cut off from the DCDC converter by an internal control pin of
 233 the DCDC converter. Thanks to the memory being non-volatile, it only has to be turned on during
 234 access and can kept turned off otherwise. A memory handling system which uses the SoC RAM
 235 whenever possible and only when necessary accesses the NVRAM is implemented in software to allow
 236 minimum on-time for the NVRAM.

237 Figure 5 shows a current measurement of the BATS mobile node. The measurement has been
 238 conducted in the lab without other mobile nodes or ground stations being present. The current was
 239 recorded with a Keysight N6705B power analyzer equipped with a precision source.

240 The peaks marked **A** occur every two seconds. They show the current consumption during
 241 calculating and transmitting the encounter data. This includes sending the OOK modulated wake up
 242 pattern as well as the FSK modulated transmission of the node ID. During all this the system is active
 243 for 8 ms. **B** corresponds to the mobile node turning on its receiver to listen if a base station is in range.
 244 If one is in range the node transmits stored data to the station. Otherwise (like seen in the plot), if

274 also collected. For better interpretations, a rough estimation on the distance in between both bats, the
275 maximum RSSI value is logged. All nodes are sending out a so-called Mobile Node Beacon (MNB)
276 periodically which contains an wakeup-sequence and an unique identifier. In order to detect the
277 presence of another bat in communication range, the wakeup-receiver is used. Once a MNB is received,
278 the *Encounter-Detection* is invoked. This module looks up whether a MNB of this particular bat has
279 been received recently and updates the values accordingly if this is the case. If no meeting is detected,
280 the *Memory Subsystem* is used to allocate new memory to store the new meeting. Every second, the
281 *Encounter-Detection* looks up, if five MNBs in a row were not received. If such kind of meeting is found,
282 we consider the meeting as closed and push it into the memory in a first-in first-out memory, which
283 then awaits transmission.

284 The *Memory Subsystem* is used to manage two different memory types, the internal Static Random
285 Access Memory (SRAM) and the external NVRAM. If memory should be allocated, the internal SRAM
286 is used to store data. This reduces overheads in terms of energy, as the NVRAM can be turned off as
287 long as possible. However, if data should be stored on NVRAM, software transactions are used to
288 prevent any corruptions of stored data due to transient failures like resets or power outages. This gives
289 us the opportunity to store data among system resets.

290 If enough meetings were logged, the *Erasure-Code* module is invoked. The purpose of this module
291 is to increase reliability of transmitted data by adding redundancy. In our case, we use a fixed code rate
292 in which two meetings are encoded. Due to the erasure coding and our chosen code rate, 2 redundant
293 packets are generated. The two redundant and two original packets are transmitted to a base station
294 eventually. These four packets are later on called chunks, as a chunk plays a central role. Out of four
295 packets in a chunk, all data can be reconstructed if at least two packets were received. Regardless of
296 the pattern of received packets, using erasure-codes offers a better performance compared to simple
297 duplication in terms of reliability.

298 The *Interleaver* is used to increase energy efficiency of the transmitted data. As the *Erasure-Code*
299 adds redundancy, we interleave packets from different chunks to decrease overheads like starting
300 the transmitter to a minimum. Thus, up to 35.14% of energy can be saved by an increased data rate
301 while only negligible reliability is sacrificed. This module, has been tested intensively theoretically
302 and practically in multiple field tests, which is beyond of scope in this paper.

303 The last module inside the data path is the *Base-Station Handler* and decides whether a data
304 transmission should be initiated and when. Depending on the current location of the bat or the node,
305 the medium access is altered. This is, because if a bat is flying past a base-station, data transmission
306 should be initiated with low latency to ensure a reliable communication. On the contrary, inside
307 the roost many nodes may send data to a base-station. As the bats are not moving inside the roost
308 and due to the high communication effort it is beneficial to send data in a Time Division Multiple
309 Access (TDMA)-alike scheme. In order to detect the presence of a base-station, so-called Base Station
310 Beacon (BSB)s are sent in a high frequency to the mobile node. Therefore, turning on the receiver can
311 be done only for short times, which saves energy on the mobile node. The BSB contains data like the
312 current configuration, the location and synchronization parameters which enables the mobile node to
313 synchronize to the base-station.

314 The last module inside the application is the *Configuration Handler* and *Status Collection*. In order to
315 ensure to alter a configuration only when no data is invalidated, the *Configuration Handler* keeps track
316 of the whole application. With the reconfiguration, we are able to alter communication parameters like
317 RSSI thresholds or timeouts. Furthermore, to monitor the whole system after deployment, we also
318 collect statistics of the system like memory utilization or time of activity. This gives us the opportunity
319 to alter the configuration, if unpredictable issues arises like exhausted memory. If nodes are acting
320 inappropriate, changing the configuration is the only way, as no reprogramming is possible after
321 deployment.

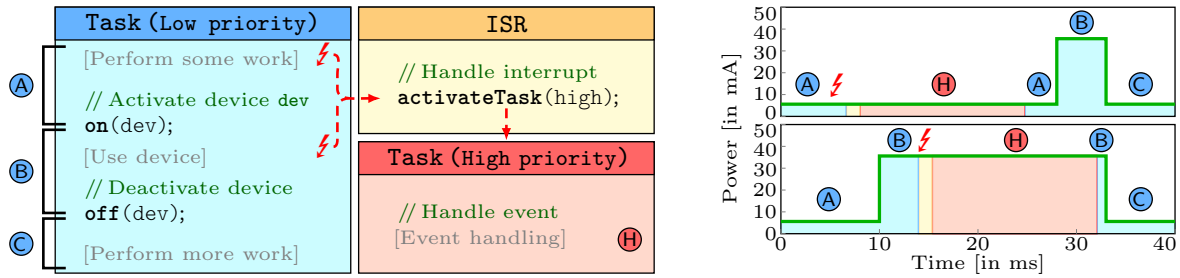


Figure 7. To determine upper bounds on the energy consumption of operations (i.e., execution of tasks) on the mobile node, temporarily activate devices and interferences of interrupts need to be considered.

3.2.2. Static Resource Analysis

Energy management on the battery-operated mobile node is crucial in order to enable a sufficient lifetime for biological experiments. In order to estimate the lifetime, we developed analysis techniques to determine the worst-case energy consumption (WCEC) of operations (e.g., execution of specific tasks) [21,22]. These estimates are not only useful for the node's lifetime estimation, but also to guarantee the completion of tasks, for example, when storing data to the available NVRAM.

The core challenges for the determination of WCEC estimates in the BATS scenario are twofold, that is, 1) dealing with temporarily activate devices and 2) considering interferences by concurrent activities in the analysis (i.e., possible interrupts, tasks with higher priority). Figure 7 exemplarily outlines these challenges: a task of lower priority temporarily activates a device (e.g., the transceiver) and thereby leads to an increase of the node's power consumption. In this scenario, an asynchronous interrupt can interfere the low task's execution. Depending on whether the interrupt occurs within the low task's duration of the activated device, the energy consumption significantly varies. The right part of Figure 7 illustrates these possible scenarios (i.e., high-power phase w/o interrupt). A safe WCEC analysis has to consider both scenarios and, in order to avoid unnecessarily pessimistic analysis results, has to precisely respect the phases where the device is switched off.

To solve these problems, we developed an analysis technique that captures phases of temporarily active devices and possible interferences in the context of the BATS projects [22]. In the first step of the analysis, we decompose the application code into blocks with a common set of active devices (see parts (A), (B), and (C) in Figure 7). Using these decomposed blocks, we carry out an explicit path enumeration of all system-wide program paths that includes all interrupts and possible task switches. With knowledge of all possible paths, we formulate an integer linear program, whose solution eventually determines the upper on the energy consumption of the analyzed task.

3.3. Received Signal Strength-based Localization

Recently, received signal strength (RSS)-based direction-of-arrival (DOA) estimation techniques gained more attention in the research community. Several power-based approaches to direction finding have been published in literature. These may use multiple directional antennas [23,24], a single rotating antenna [25,26] or active reflectors [27]. An alternative opportunity, instead of mechanically moving the antenna, is the use of switched beam antennas as presented in [28] and [29]. Another approach is applying electronically steerable parasitic array radiator antennas, as presented lately in [30]. Recently, multi-mode antennas have been investigated for power-based DOA estimation [31]. Also a variant of the MUSIC algorithm for power measurements has been proposed in [32]. Theoretical limits in RSS-based direction finding have been discussed in [24].

For this paper we consider RSS-based DOA estimation applying coupled dipole antennas [33]. Furthermore, it is assumed that localization takes place in the horizontal plane orthogonal to the two dipoles. Presuming a perfect linear dipole array, the radiation of the dipoles in the horizontal plane

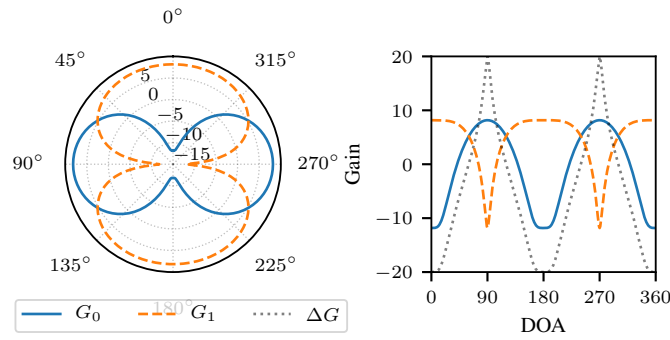


Figure 8. Radiation power patterns for perfect dipole antennas in horizontal plane for in phase and out of phase coupling.

(i.e., $\theta = 90^\circ$) is constant over all impinging signal angles in azimuth $\phi \in [0, 2\pi]$. Hence, the radiation pattern for N dipoles is given by the array factor [34] $AF = \sum_{i=0}^{N-1} c_i \cdot \exp(-j \cdot 2\pi \sin(\theta) \cdot d_i \cos(\phi))$, where d_i are the corresponding distances of the dipole elements, λ is the wavelength, and c_i is the coupling factor. Considering only two dipoles at distances $d_0 = 0$ and $d_1 = d$ and $\theta = 90^\circ$ the array factor reduces to $AF = c_0 + c_1 \cdot \exp(-j \cdot 2\pi \cdot d \cos(\phi))$.

For the considered antenna array the dipoles are coupled in phase and out of phase, respectively. Hence, the radiation patterns are given by [24] $g_0(\phi) = 1 + \exp(-j2\pi d \cdot \cos(\phi))$, and $g_1(\phi) = 1 - \exp(-j2\pi d \cdot \cos(\phi))$. We define the radiation power patterns $G_a(\phi)$ (in dB) by $G_a(\phi) = 10 \lg |g_a(\phi)|^2$. The gain difference function of the described antenna array is expressed by

$$\Delta G(\phi) = G_1(\phi) - G_0(\phi). \quad (1)$$

The radiation power patterns for the antenna array at hand and the gain difference function are depicted in Figure 8.

The RSS at a receiver a for a transmitted signal with power P_{TX} can be computed as follows $P_{RX,a} = P_{TX} - L + G_{TX} + G_a(\phi)$, with L denoting the bulk path loss. G_{TX} and $G_a(\phi)$ are transmit and receive antenna gain, respectively. When considering a single signal source, i.e., no multipath propagation, the received signal strength difference is given by

$$\Delta P_{RX} = \Delta G(\phi) + w, \quad (2)$$

due to the fact that both channels are stimulated by the same transmit power and exhibit equal path loss. Thus, the gain difference function does not depend on transmit power and path loss. Hence, it may be estimated without prior knowledge of the the path loss exponent and the power emitted by the transmitter. This fact is, in contrast to range-based localization based on RSS, a major benefit of RSS-based DOA estimation. The above consideration hold for the absence of multipath propagation. In case of multiple multipath components (MPCs) the observed difference in signal strength is not linked to the DOA of the line-of-sight (LOS) component.

For an improvement of the localization accuracy every localization sensor node utilizes two frequencies. The developed antenna for our application is presented in [33] and has two orthogonal antenna pattern for the frequencies 868 MHz and 2.4 GHz. Due to the large frequency distance the fading of the two frequencies can be assumed as uncorrelated. In Figure 9 a block diagram of a localization sensor node is shown. The antenna array is connected to a RF-frontend which receives at 868 MHz and 2.4 GHz simultaneously with two channels. In the Field Programmable Gate Array (FPGA) of the processing platform the signal detection is performed by correlation to the preamble and sync word of the mobile node signal like presented in [33]. The detected signal is processed by the microcontroller where a frequency estimation and correction is performed to decode

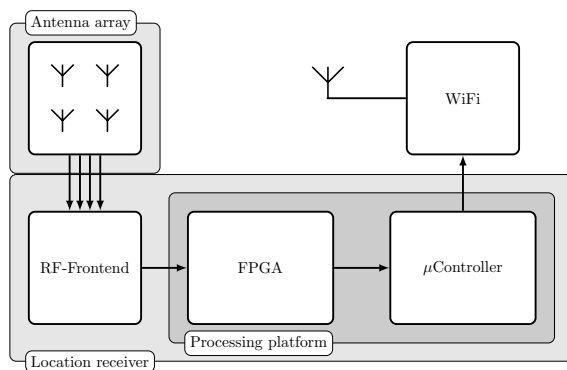


Figure 9. Block diagram of sensor node.



Figure 10. Localization receiver.

381 the bat ID and data. In Figure 10 a picture of a localization node is shown. During operation the
 382 antenna and receiver is covered with a housing.

383 3.3.1. Optimal Design of RSS-based DOA Sensors

384 As the classical performance measures, such as the Cramer-Rao Lower Bound (CRLB), are not
 385 capable of considering ambiguities in DOA estimation, power-based DOA estimation sensors are
 386 reviewed from an information-theoretic view in this section. The basic idea is find a antenna geometry
 387 that maximizes the information gained from a RSS measurements [35]. Recently, there has been a
 388 revival of information theory in many fields. Information-theoretic measures, have been utilized, just
 389 to a name a few of them, to optimize MIMO radar waveforms [36], to quantify the loss in sub-Nyquist
 390 sampling [37,38], and to compute fundamental limits in compressed sensing [39] and bounds for
 391 kernel-based time delay estimation [40]. Utilizing the framework of information theory this can be
 392 achieved maximizing the mutual information. Maximizing the mutual information, i.e., the total
 393 information gained from a sensor measurement, is by far more generic than local precision measures,
 394 such as the CRLB. Thus, in contrast to the CRLB, information-theoretic measures are applicable in case
 395 of multi-modal or non-Gaussian probability densities [35].

396 Compared to the most common approach directly inferring DOA from phase differences, such
 397 as uniform linear antenna arrays, in RSS-based DOA estimation coupling between antenna elements
 398 is used to realize angle dependent gain patterns. This can be thought of as static beam forming. The
 399 benefit of this approach is that DOA of the impinging signal results in an RSS change at the receiver.
 400 Hence, DOA estimation is feasible with non-coherent receive channels. From an economical point of
 401 view this is very beneficial since non-coherent receiver may be manufactured at low cost compared to
 402 phase-coherent receivers. A realization of such a low-cost tracking system has been presented in [33].

403 The major challenge is the design of the antenna radiation patterns of such a localization system.
 404 The shape of the antenna pattern is defined by the geometrical arrangement of the antenna elements, the
 405 gain pattern of the elements and the combination of the signals. In the sequel, the mutual information
 406 of a DOA measurement considering the BATS antenna is computed. The following setup is considered.
 407 Localization takes place in the horizontal plane. The antenna array consists of two dipoles that are
 408 orthogonal to the plane, i.e, $\vartheta = 90^\circ$. The two dipoles are coupled in phase and out of phase for the
 409 two antenna ports as described in the section above and the gain pattern as described in Section 3.3.
 410 Previously a distance between the dipoles of $d = \lambda/2$ was considered. In this section, the distance d
 411 is the design parameter of the antenna array to be optimized. The criterion to be maximized is the
 412 mutual information. In other words, the distance with the maximum total information gain is sought.

413 In a nutshell, the following procedure needs to be carried out in order to derive the optimal array
 414 geometry for power-based DOA estimation.

- 415 1. Compute radiation patterns for distance d

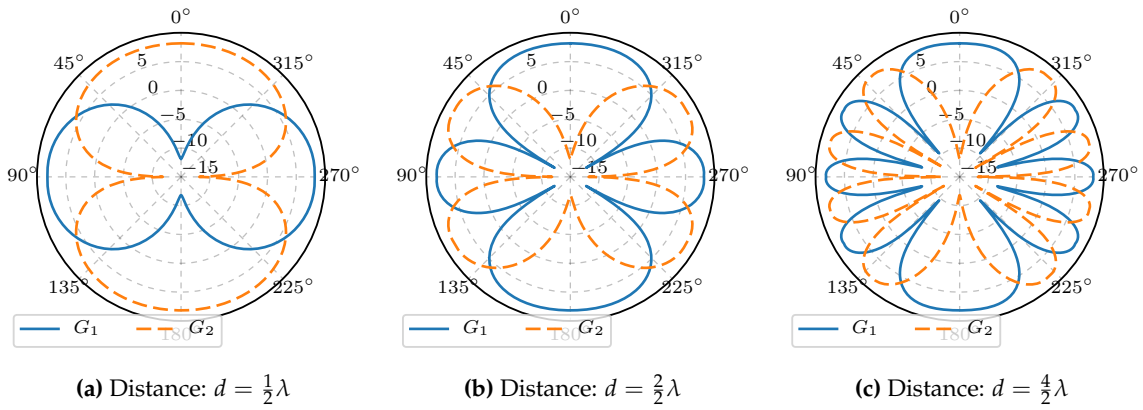


Figure 11. Radiation power patterns for antenna arrays with different dipole distances.

- 416 2. Derive measurement function, i.e., the gain difference function ΔG
- 417 3. Compute posterior probability density function (PDF) and joint PDF
- 418 4. Compute entropy

419 Radiation power patterns for different distances between the two dipoles are shown in Figure 11.
 420 Obviously, the in phase and anti-phase feeding results in orthogonal radiation patterns. Furthermore,
 421 it is easy to recognize that an increasing number of lobes results in an increasing gradient of the gain
 422 difference function ΔG . That in turn leads to a decrease in the estimation variance in presence of
 423 measurement noise. However, on the other hand ambiguities arise.

We now consider information-theoretic measures to optimize the antenna array described above. In RSS-based DOA estimation the measurement likelihood is given by $p(\Delta P_{RX}|\phi) \sim \mathcal{N}(\Delta G(\phi), \sigma_{\Delta P_{RX}}^2)$. It is assumed that there is no prior information on the signal direction available. Hence, a non-informative prior is chosen $p(\phi) \sim \mathcal{U}(-\pi, \pi)$. With the prior the entropy before the RSS difference measurements is given by $h(\phi) = -\int p(\phi) \log(p(\phi)) d\phi$. The conditional entropy is computed as follows

$$h(\phi|\Delta P_{RX}) = -\iint p(\phi, \Delta P_{RX}) \log(p(\phi, \Delta P_{RX})) d\phi d\Delta P_{RX}, \quad (3)$$

with the posterior PDF given by $p(\phi|\Delta P_{RX}) = p(\Delta P_{RX}|\phi)p(\phi)/p(\Delta P_{RX})$ and joint PDF expressed by $p(\phi, \Delta P_{RX}) = p(\Delta P_{RX}|\phi)p(\phi)$ Finally, the mutual information is given by

$$I(\phi; \Delta P_{RX}) = h(\phi) - h(\phi|\Delta P_{RX}). \quad (4)$$

424 The mutual information quantifies the total information gained from a RSS difference measurement.
 425 In Figure 12 equation (4) is evaluated for different distances between the two dipoles. As with the
 426 phase-based direction finding the mutual information increases for distances increasing from 0 to
 427 $\lambda/2$. At a distance of $\lambda/2$ the mutual information has a maximum. Beyond $\lambda/2$ the mutual information
 428 decreases until it increases again towards a distance of λ . It can be seen that the mutual information
 429 has local maxima at distances $d = n \cdot \lambda/2$. Apparently, all local maxima have the same height. Hence,
 430 the optimal dipole distance is $d_{opt} = n \cdot \lambda/2$. In conclusion, it is possible to trade of ambiguities
 431 for local precision or vice versa without changing the total information gained from RSS difference
 432 measurements. In other words, all DOA sensors with $d = n \cdot \lambda/2$ provide exactly the same information.

433 3.3.2. Multipath-Robust Localization

434 In this section a probabilistic multipath mitigation method is presented that makes use of statistical
 435 prior channel knowledge in order to compensate multipath effects [41]. The presented mitigation

436 technique allows for mean-free DOA estimates on average if prior knowledge of the channel parameter
 437 angular spread (AS) is available. This is achieved by computing multipath adaptive power patterns
 438 for the utilized antenna arrays incorporating the AS. As mentioned in Section 3.3, bulk path loss
 439 and shadowing have no influence on the RSS difference at the receive antenna. However, multipath
 440 propagation affects the RSS difference significantly. Hence, the measured RSS difference is impaired
 441 which degrades the DOA estimation.

In general the impulse response of a wireless channel can be described by a tapped delay line [42] of L MPCs given by $h(t) = \sum_{l=1}^L a_l \cdot \delta(t - \tau_l)$, where a_l is the complex coefficient of the l -th multipath component and τ_l its respective delay. Considering the presented antenna array, the RSS difference of a received signal affected by multipath propagation can be calculated by superposition of the MPCs

$$\Delta P_{RX} = 10 \lg \left| \sum_{l=1}^L g_1(\phi_l) \cdot a_l \right|^2 - 10 \lg \left| \sum_{l=1}^L g_2(\phi_l) \cdot a_l \right|^2, \quad (5)$$

where $g_r(\phi_l)$ is the complex gain coefficient of antenna r at the arrival angle ϕ_l . With (5) the effective gain of the receive antenna for a particular realization of the multipath channel can be computed. Obviously, the angular spread significantly impairs the measured RSS at the two antennas and thus causing a bias in DOA estimation. In presence of multipath propagation equation (2) does not hold true. In multipath scenarios there is no distinct relation between gain difference and RSS difference in general, and hence

$$\Delta P_{RX} \neq \Delta G(\phi) + w. \quad (6)$$

The basic idea of mitigation technique is to derive a modified measurement function, i.e., and adaptive gain difference function $\Delta G_{MPC}(\phi)$, that allows for compensation of the multipath induced bias on the DOA estimates. For the multipath adaptive gain difference function $\Delta G_{MPC}(\phi)$ the following equation has to hold true

$$\Delta P_{RX} = \Delta G_{MPC}(\phi) + w. \quad (7)$$

442 If a gain difference function $\Delta G_{MPC}(\phi)$ can be found that fulfills (7) multipath impairments can be
 443 mitigated in a probabilistic manner. This RSS-based DOA is realized by incorporating the angular
 444 spread in the description of the antenna patterns. Such a multipath adaptive measurement function
 445 realizes a DOA estimation that has a zero-mean error on average. Therefore, the circular gain patterns
 446 are convolved with a scaled normal distribution with a standard deviation of $\sigma_{\phi_{AS}}$. Hence, the
 447 multipath adaptive measurement model is derived as follows $|g_{MPC}(\phi)|^2 = |g(\phi)|^2 * p(\phi)$, where $p(\phi)$
 448 is the PDF of the distribution of the angular spread given by $p(\phi) \sim N(0, \sigma_{\phi_{AS}}^2)$, and $(*)$ denotes a
 449 circular convolution. Note that the gain function is in non-logarithmic scale here. The resulting gain
 450 patterns are depicted in Figure 13 for different values of the angular spread. For smaller spreads the
 451 modified measurement function does not differ much from the gain difference function of the original

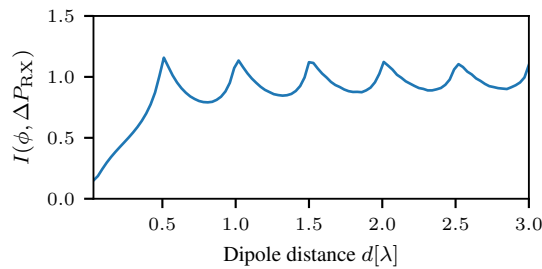


Figure 12. Mutual information of RSS-based DOA estimation for two orthogonal patterns at different dipole distances.

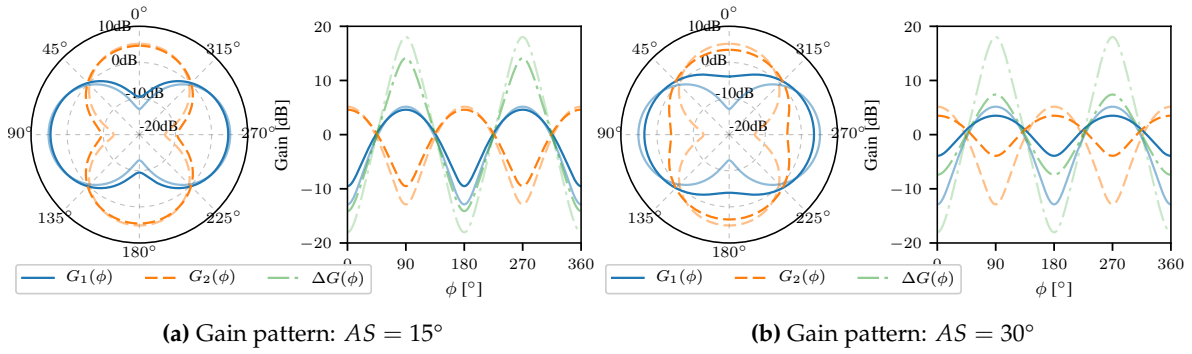


Figure 13. Multipath adaptive models describing the expected RSS difference for different values of angular spread. Dotted lines denote the original pattern.

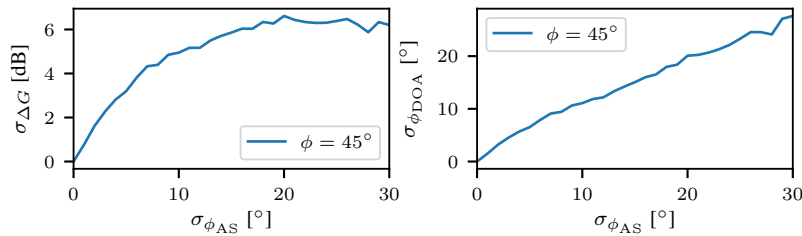


Figure 14. Standard deviation of RSS difference due to multipath propagation (left). Standard deviation of the inferred DOA estimate (right).

452 antenna patterns. Larger spreads result in flattened effective gain functions. It can be easily seen that
 453 the dynamic range of the effective gain difference function is significantly reduced due to a larger AS,
 454 i.e., the presence of multipath. Under the assumption that the channel parameter AS is known, it has
 455 been shown that probabilistic multipath mitigation allows for zero-mean DOA estimates.

456 The presented approach allows for zero-mean compensation of effects from multipath propagation
 457 [41]. However, that mitigation does not come for free and leads to an inherently increased variance
 458 in RSS difference measurements. The dependence of RSS difference standard deviation has been
 459 determined by Monte Carlo simulations and is depicted in Figure 14 for a LOS angle of 45° . Observing
 460 the results presented in Figure 14, the standard deviation for the RSS difference is saturated at mean
 461 spreads larger than 20° and resides constant at a values of ~ 7 dB. One might conclude that the
 462 variance of the RSS inferred DOA also does not increase with larger angular spreads. However, that is
 463 a false conclusion. The multipath adaptive gain difference function flattens with increasing angular
 464 spread (cf. Figure 13) which results in a decreasing gradient of the function $\Delta G_{MPC}(\phi)$. Thus, the
 465 variance of the DOA estimate increases according to the linear transformation of the variance from
 466 measurement domain to parameter domain $\sigma_{\phi_{DOA}}(\phi_0) \approx \Delta G^{-1}(\phi_0) \cdot \sigma_{\Delta P}(\phi_0)$. Hence, with increasing
 467 mean angular spread even for a constant variance in RSS difference the variance in DOA estimates
 468 increases. The proposed multipath mitigation technique enables for unbiased DOA estimation in
 469 multipath scenarios with known mean angular spread. However, the mitigation comes at an expense
 470 of an increased variance in DOA estimates.

471 3.4. Long Range Telemetry

472 As already addressed in Section 3, the ground network enables the download of encounter data,
 473 so-called *meetings* and provides a precise localization of bats in the close-up range. However, the
 474 trackable region is limited to the area covered by the base station network. The usage of additional

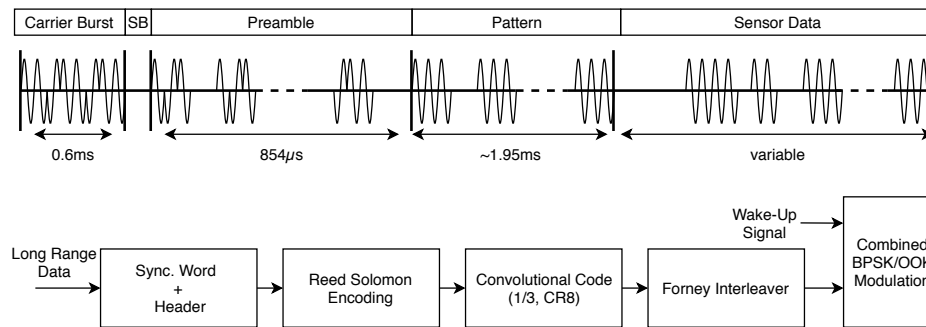


Figure 15. Combined modulation of long range telemetry data utilizing the wake-up burst showing the corresponding waveform and encoding scheme.

475 stations is costly, both in acquisition and operation effort. With the bats flying at high speed, they
 476 are likely to leave this region within a short period of time, especially when hunting. While no
 477 high-resolution tracking can be provided outside the ground network, the bats shall still be observable
 478 by the system even in distances of several kilometers to enable a long-term monitoring. To tackle
 479 this challenge, a dedicated system of distributed telemetry base stations was established, forming
 480 a Low Power Wide Area Network (LPWAN). Theoretical analysis [43] as well as field results [44]
 481 demonstrate, that low rate sensor data like bat identification, air pressure, 3D-acceleration or other
 482 sensor data can successfully be received kilometers beyond the ground localization network (see
 483 Section 4). In the following, we briefly illustrate the system components and algorithms implementing
 484 the long range telemetry transmissions.

485 3.4.1. Long Range Telemetry Transmission Scheme

486 For low power long range data transmission there are already systems like LoRa or Sigfox
 487 available. However, LoRa as well as other systems require sending dedicated packages for long range
 488 communication. The transmitter nodes are limited both in size and weight since the bat is not capable
 489 to carry larger batteries. Therefore, incorporating a long range telemetry scheme is imposing rather
 490 contradictory requirements on the system since no additional hardware or energy source should
 491 be added. However, an additional long range transmission shall be implemented. Therefore the
 492 BATS project makes use of already transmitted packages rather than adding an additional ones. The
 493 encounter detection in the BATS project (see Section 3.1.3) is performed utilizing an OOK modulation
 494 scheme with limited range. When this, so-called wake-up signal (*cf* Fig. 3, component *WuRX*), is
 495 received by another bat near by, it triggers its processor to return from deep sleep mode for an exchange
 496 of bat IDs and metadata, noted as encounter or *meeting*.

497 In order to embed the telemetry transmission into the existing system, we perform a combined
 498 modulation of OOK-modulated wake-up bits together with a Binary Phase Shift Keying (BPSK)
 499 modulation for encoding the telemetry data using two BPSK bits per OOK bit. This way additional
 500 packages are omitted and the energy efficiency of the developed long range scheme is far more efficient
 501 than state of the art systems that require their own packages. Figure 15 depicts the encoding scheme
 502 and waveform for the telemetry transmission proposed, to cope with the harsh restrictions on energy
 503 and weight.

504 As can be seen in the upper part of the Figure, the OOK-modulated signal is alternated in its
 505 phase at distinct sample instances. This is done during the carrier burst and preamble of the wake-up
 506 pattern (*cf* Fig. 15), as these sequences are common to all bat nodes, fixed in length and structure
 507 and also the on-times are known. The pulses are Manchester-coded to eliminate any dependency
 508 between the number of on-times and the data transmitted within the wake-up signal. This allows for
 509 an efficient exploitation of this OOK scheme for implementing the long range telemetry transmission

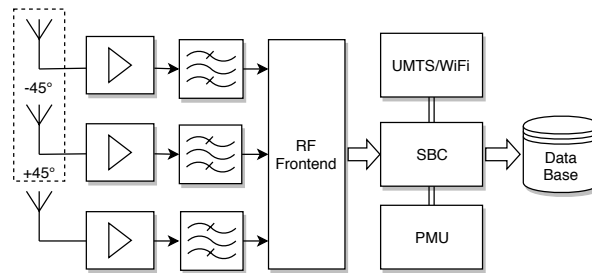


Figure 16. Simplified block diagram of the long range telemetry base station architecture.

510 without supplementary hardware or an additional expenditure of energy, as the phase is not used by
 511 the wake-up itself.

512 For a successful decoding even in large distances, a sophisticated encoding must be applied.
 513 Following the lower part of Fig. 15, the long range payload data is extended by a synchronization word
 514 and header information carrying the bat ID among other information. Error detection is performed
 515 by means of a shortened Reed-Solomon Code RS(253,255) in combination with a convolutional code
 516 (0255,0331,0367) exhibiting a code rate of $\frac{1}{3}$ and a constraint length of 8. A Forney interleaver with
 517 24 branches distributes one payload byte over 24 wake-up bursts, resulting in a time interleaved
 518 transmission of each long range telemetry packet of almost one minute. This approach adheres
 519 to the idea of the so-called *Telegram Splitting* concept as presented in [45,46]. Thereby, information
 520 is spread within the time (and frequency) plane in a burst-like fashion. As the bat nodes operate
 521 in the unlicensed Short Range Devices (SRD) band around 868 MHz, this technique is eligible to
 522 mitigate the influence of the channel and other interferers, as experienced in earlier measurements [47],
 523 thus assuring an ultra-robust transmission in combination with the Forward Error Correction (FEC)
 524 algorithms presented. Given this encoding, we obtain a nominal payload data rate of 11.363 kbit/s
 525 for the telemetry modulation scheme. Accounting for the duty cycle (wake-up burst length of about
 526 3 ms) along with the error coding overhead, one results in 1 absolute payload byte per burst or a
 527 rate of about 4 payload bits per second (under the presumed configuration of a 2 s burst interval).
 528 Thus, a low rate and robust long range telemetry transmission is implemented, capable of transferring
 529 periodically gathered sensor data without the need for additional energy or any system changes, except
 530 for software.

531 3.4.2. Telemetry Base Station Architecture

532 For an optimal system performance also the receiving network has to be properly designed. In
 533 [43] we presented theoretical analysis of the achievable transmission range related to rate and the
 534 environment scenario modeling the radio channel. Depending on the height of the transmitting bat
 535 nodes and the receiving base stations, one has to overcome path losses of more than 150 dB in distances
 536 of 5 km, while supporting data rates of just a few bit/s for a balanced relation of energy expenditure
 537 per telemetry bit. This finding is in compliance with our system layout as described in Section 3.4.1.
 538 To alleviate the influence of shadowing obstacles like trees, the base stations, forming the long range
 539 telemetry reception network, are located at exposed sites around the habitat of bats. Measurement
 540 sites on roof tops or towers assure an almost line of sight connection to the bats when flying. Figure 16
 541 shows a simplified signal processing chain of a telemetry base station.

542 The station is equipped with three antennas in total, where one is a directional antenna internally
 543 consisting of two cross-like antenna arrays rotated against each other (*cf* $\pm 45^\circ$). These antennas exhibit
 544 with a high average gain of 14 dBi at a half-power beam width of 66° to counteract the high losses to
 545 be expected. A third omni-directional antenna with 0 dBi assures a gap-less spatial reception coverage.
 546 This Multiple Input Multiple Output (MIMO) like architecture enables means of stream combining
 547 and beam forming to mask interferers and further improve the decoding rate. Each reception stream is

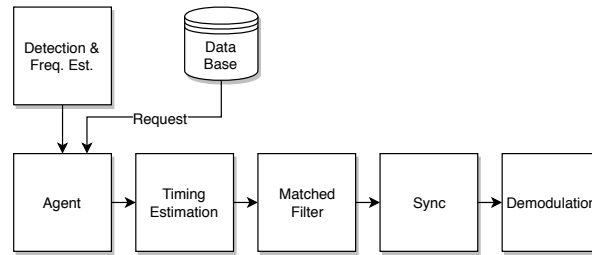


Figure 17. Offline demodulation process of long range telemetry data.

548 fed through a Low Noise Amplifier (LNA) and a half-band filter cascade, before being digitized by a
 549 self-developed radio frontend. A C++ driven Software Defined Radio (SDR) framework [48], hosted by a
 550 single board computer (SBC), performs signal processing before compressing and storing the In-Phase
 551 and Quadrature (IQ) data to a local persistent storage. An Universal Mobile Telecommunication
 552 System (UMTS) modem provides means for remote control, while the Power Management Unit (PMU)
 553 controls the discharge and recharge process via solar panels of the station's batteries, allowing for an
 554 autonomous and self-sustaining operation.

555 Figure 17 illustrates the demodulation process of the gathered data. With 3 data streams, each
 556 exhibiting a sampling rate of 2 MHz and a resolution of 12 bit for in-phase and quadrature component,
 557 respectively, the resulting transfer rates for streaming the recorded data to a remote storage via the
 558 internet would be costly and would constitute a bottleneck for the digital signal manipulation. The
 559 signal processing chain has to cope with these high rates to avoid data loss by buffer overflows.
 560 Therefore, the demodulation is performed offline. With the vast amount of raw IQ data, a direct
 561 search for telemetry signal bursts would be both, time and computationally intensive. To alleviate
 562 this problem, we implemented a so-called *Agent* (cf Fig. 17). This software module is instantiated for
 563 each bat signal, detected by a preceding detection algorithm. We exploit the periodicity of bursts²,
 564 such that when a signal once has been discovered, the *Agent* can make concise requests to a database,
 565 rather than loading and traversing complete streams. The database in turn provides metadata, such as
 566 a precise Coordinated Universal Time (UTC) timestamp, that eases the access, following the periodic
 567 burst sequences in time intervals of several seconds. Subsequently, a multi-stage timing and frequency
 568 estimation are carried out, followed by matched filtering, synchronization and the demodulation
 569 process.

570 This section briefly illustrated the long range telemetry functionality. The new transmission
 571 scheme was successfully integrated into the existing system without the need for additional hardware
 572 on the sensor nodes or an increased energy consumption. We presented both, the introduced telemetry
 573 base stations as well as the software components running the transmitter and receiver side. First
 574 measurement results are given in Section 4, to prove the long range functionality in a practical setup.

575 3.5. Data Backend

576 Meeting data must be cleansed before analysis. There is an inconsistency between the recorded
 577 meeting data and domain knowledge. On a semantic level meetings between tracked objects are
 578 reflexive, i.e. if object 5 has met object 7, object 7 also must have met object 5. However, often the
 579 counterparts are missing in the recorded data.

580 Another issue is a classification issue. If other means are not available, the position can be deduced
 581 from the number of simultaneous meetings. Trajectories are measured in an a priori determined area

² As described in Section 3.4.1, the long range data is structured in packets that are distributed over several wake-up bursts and encoded within phase changes. Therefore, only after the demodulation of several subsequent bursts, one complete telemetry packet is retained again (compare *Telegram Splitting* technique).

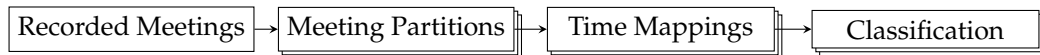


Figure 18. Overview of the Data Backend Processing Steps

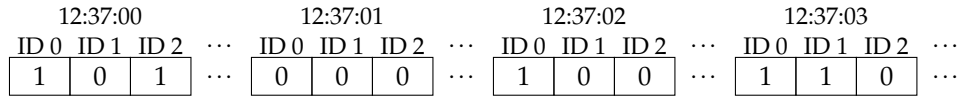


Figure 19. Memory Layout of the Mapping from Time to the Set of Encountered Ids

582 of interest and are thus not usable to determine positions outside of this area. We often used the ID of
 583 the base station which received the meeting data to deduce locations. But in some scenarios, it is not
 584 feasible to install a base station at certain locations, because they are not known a priori, or they are
 585 simply hard to reach. In the case of bats, one very interesting location is the roost. We expect more
 586 generally, that locations of assemblies are interesting in most scenarios. Even if we cannot determine
 587 the exact location of an assembly, it is still valuable to know when a tracked object participated in an
 588 assembly. To do this, we use the number of simultaneously met objects to decide whether an object
 589 was at an assembly or not.

590 Figure 18 illustrates these computational steps. All steps can be performed in parallel for each ID.
 591 This is indicated by shadows.

592 3.5.1. Implementation

593 To solve the inconsistency issue, either meetings lacking their reflexive counterpart must be
 594 removed or the missing counterparts must be added. As the meeting detection does not create false
 595 positives, adding missing values is the correct approach.

596 However, instead of physically adding missing counterparts to the data set, we make use of the
 597 fact, that the data must be partitioned for later classification anyway. During partition creation, we use
 598 all reported meetings involving the current ID of interest regardless of the reporters' IDs, and thereby
 599 erase the information of origin. This results in one consistent table of possibly overlapping meetings
 600 for each ID.

601 The next step is to create a mapping from time to the currently encountered ids for each object.
 602 This implicitly removes the redundancy created by overlapping meetings. We represent this mapping
 603 by creating an appropriately sized array of bitsets. Each bitset represents a second, each bit in the bitset
 604 corresponds to an ID of a potential meeting partner (cf. Figure 19).

605 As the data set contains a lot of noise, the results are smoothed by considering windows of
 606 user-specified size centered around each second. The results are stored in a second array which content
 607 is the union of all bitsets in the corresponding window. This is implemented efficiently by virtually
 608 shifting the input array by offsets and using the bitwise-or operation to implement the set-union.

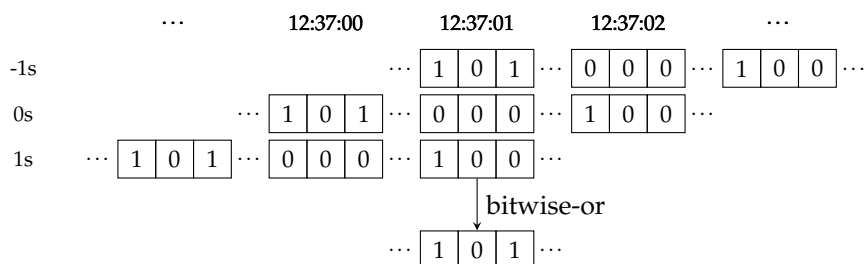


Figure 20. Union Operations for a Two-Second Window

609 Figure 20 illustrates this operation by continuing the example from Figure 19 for a two second window
610 around 12:37:01. Finally, the assembly classification is done by comparing the number of set bits to a
611 specified threshold.

612 3.6. Diversity Combining for Improved Communication

613 Whenever a bat equipped with a sensor tag visits the hunting ground, the stored contact
614 information needs to be transmitted down to the deployed ground network. As the communication
615 takes place in a forest environment, the signal is not only affected by Free Space Path Loss (FSPL) and
616 multi-path fading, but, additionally, by shadowing from trees that lie in between. Furthermore, due to
617 the fast movement of bats and low transmit power of the sensor tag, there is a need of techniques that
618 offer increased communication reliability. Since there are already multiple base stations available in
619 the ground network for localization purposes, there is a high probability that the signal transmitted by
620 the bat sensor tags will be received by multiple of these base stations. Therefore, we propose to use
621 these base stations in the ground network as a distributed antenna array to apply receive diversity
622 combining for an improved reception.

623 Using spatially separated antennas on the receiver side to perform diversity combining is one
624 of the most popular and cheap techniques to combat fading. The most commonly used diversity
625 combining techniques include Maximum Ratio Combining (MRC), Equal Gain Combining (EGC), and
626 Selection Diversity (SD) [49]. On the one hand, MRC and EGC provide the highest diversity gain but
627 that comes with an expense of increased processing demands. For example, to perform constructive
628 combining, all branches are weighted (unity for EGC and relative to their received Signal to Noise
629 Ratio (SNR) for MRC), aligned, and co-phased before addition. While on the other hand, SD selects a
630 branch with the highest SNR and, hence, does not require a complex algorithm but the diversity gain
631 achieved is also minimal compared to the others.

632 Such a distributed antenna system also helps to make the system becomes more robust against
633 not only multi-path fading but also shadowing [50]. This concept is similar to macro-diversity used in
634 cellular networks in which multiple base stations connected to each other via optical fiber cooperatively
635 decode the same signal to increase the RSS [51]. In our system, nodes in the ground network are
636 connected to each other through wireless connections, hence, it imposes limit on the maximum data
637 rate that is achievable to exchange the information between nodes to perform diversity combining at a
638 single point.

639 One option to successfully forward data from all base nodes to a sink node is to process the
640 received data at nodes locally and forward soft-bits only [52]. Since soft-bits contain only one float
641 value for every single bit, the information that needs to be forwarded reduces dramatically, hence,
642 the network is not overloaded. The sink node combines soft-bits instead of signal samples, which
643 certainly increases the RSS, however, the diversity gain achieved is not the highest because the system
644 loses signal properties while converting the signal into soft bits [53]. As an alternative, we propose the
645 concept of selective signal sample forwarding [54]. In the proposed approach, all base nodes detect
646 the received signal copy locally by correlating the incoming samples with the known preamble. In
647 the case of detection, channel parameters such as phase information is estimated also through the
648 preamble and compensated for constructive combining. The local nodes then slice the signal starting
649 from preamble equivalent to the known packet length and forward only these relevant I/Q samples to
650 the sink. As multiple bats can transmit with a maximum rate of 100 Hz, a packet size of less than 1 ms
651 reduces the data rate required in the ground network by more than 10 times and, thus, resulting it in
652 the range of few Mbit/s. Finally, the sink node receives all locally detected signal copies and applies
653 diversity combining on the received I/Q samples. The performance achieved with the selective signal
654 sample forwarding is the same as achieved with the conventional diversity combining and degrades
655 only if the local base nodes do not detect the signal successfully [54].

656 To analyze the performance of our proposed approach, we implemented the BATS transmitter and
657 base nodes receiver in GNU Radio, an open source signal processing tool to implement the software

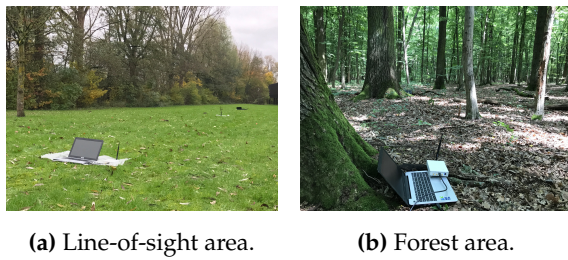


Figure 21. Types of areas to conduct diversity combining experiments.

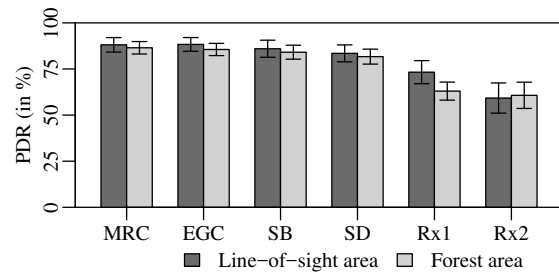


Figure 22. Packet delivery ratio achieved with different diversity combining techniques in realistic environments.

part of a radio. We validated our implementation by conducting an extensive set of simulations and over-the-air lab measurements. The implementation and validation details are explained in [55]. As a step further, to test our model in realistic environments, we performed a series of outdoor experiments in LOS and forest areas as shown in Figure 21. To conduct experiments, we use two Ettus B210 Universal Software Radio Peripherals (USRPs) as receivers and one as a transmitter all connected to laptop computers. We placed both receivers 30 m apart and moved the transmitter at a human walking speed, i.e., 4 km/h to 5 km/h, between the receivers in such a way that its distance from both receivers always remains equal during an experiment in both areas. The maximum transmit power of B210 USRP is in the range of 10 dB m, however, since the USRPs are not perfectly calibrated, we fixed the transmit power by adjusting the gain in a way that the average Packet Delivery Ratio (PDR) at a single receiver stays better than 50%. We recorded the data of each receiver to apply various diversity techniques with exact same channel conditions and processed it offline.

Figure 22 shows the PDR achieved at each individual receiver, i.e., Rx1 and Rx2, as well as results for the different diversity techniques. The error bars depict the 95% confidence intervals and are obtained by repeating the experiments 30 times. As SNR in the resultant signal in MRC is the linear combination of SNRs of individual signal copies, it provides the best performance, i.e., achieves a PDR of 88% and 86.5% in LOS and forest area, respectively. EGC performs only marginally worse than MRC despite the fact that EGC involves relatively less processing to calculate the gain values. This happens due to the fact that only two receivers or branches are involved with roughly similar SNR. The difference between MRC and EGC is more prominent if higher numbers of branches contribute for diversity combining. Successful Branch (SB) represents the performance of a system in which a reception is considered successful if any of the base nodes decode the signal correctly without any combining. SB performs inferior to MRC as well as EGC and achieves a PDR of 86% and 84% in LOS and forest area, respectively. Nevertheless, the performance of SB is about 2.5% better than SD in both areas. Hence, it can be stated that selecting the highest average SNR branch for SD does not always help in decoding the best signal because sometimes the same average SNR of two different signals lead to different outcomes because of their different instantaneous SNRs. Regardless of diversity technique used, it is clear that using base nodes in the ground network as a distributed antenna array for diversity combining improve the communication reliability. Moreover, the performance is analyzed here for a two-branch diversity system only and the improvement is still evident. In the final setup, we aim to use multiple base nodes for diversity combining and, hence, further improving the diversity gain.

4. System Verification

The current system has been thoroughly tested by tracking free-ranging bats of several species. During field deployments, researchers may adjust the complexity of the deployed system according to their research question, while either the full functionality (e.g., tracking, encounter detection, long-range telemetry for studying foraging behavior) may be used or only subsets (e.g., encounter

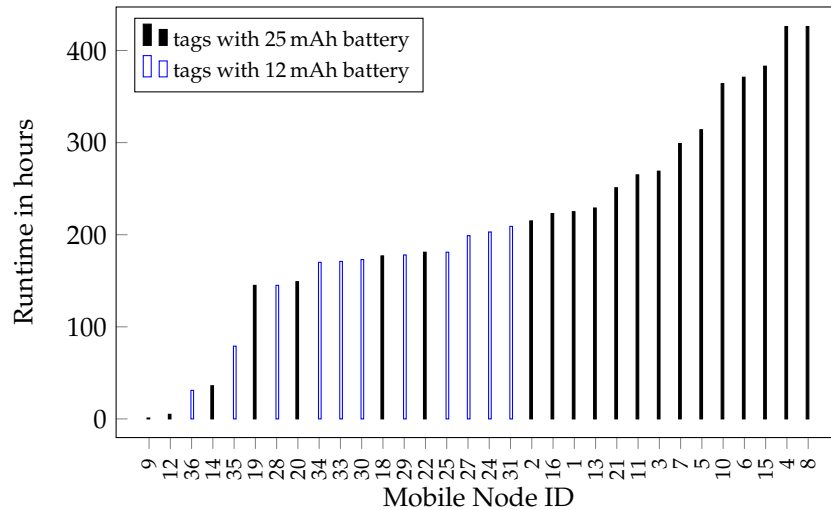


Figure 23. Runtime of each node in hours

694 detection and long-range telemetry for studying social behavior). These two scenarios have been tested
 695 in Forchheim, Germany, and Berlin, Germany, respectively, in the following referred to as "Forchheim
 696 field test" and "Berlin field test".

697 4.1. Runtime

698 Differences in individual behavior causes significant variation in energy demand and battery life.
 699 Particularly when individuals spend considerable time within the ground station network, which leads
 700 to an increase in sampling rate, the power consumption is increased. The runtime of the mobile nodes
 701 deployed in the Berlin field test is shown in Fig. 23. Here batteries with 15 mAh respectively 25 mAh
 702 have been used according to the maximum acceptable weight for the corresponding individuals.

703 The runtime has been calculated from the first to the last radio contact to each node. This includes
 704 direct contact to a base station and also encounters between tagged animals. A low runtime can be
 705 explained by the corresponding animal leaving the covered area and thus preventing the mobile node
 706 to be received by any other sensor network node or base station. With small (12 mAh) batteries a
 707 runtime of up to 209 h (nearly 9 days) and with big (25 mAh) batteries a runtime of up to 426 h (nearly
 708 18 days) has been recorded. On average the sensor tag draws a current of 55 μ A. This includes a low
 709 power sleep state with enabled wake-up receiver as well as periodic wake-ups to send out beacons
 710 every 2 s and check for base station contact to transmit the stored data. A slower beaconing frequency
 711 would lead to a reduced energy consumption but would also decrease the time resolution of recorded
 712 encounters and in turn increase the risk of missing short encounters. During the runtime seen in Figure
 713 23 a total of 60.000 meetings have been recorded and 2.7 million received pseudo localization beacons
 714 have been recorded. These pseudo localization beacons are used to give a rough location of the animal
 715 based on which base station can receive the beacons.

716 4.2. Trajectories

717 The localization methods presented in section 3.3 were validated during the Forchheim field
 718 test in summer 2017. The localization network at the test site was operated for 18 days with 17 fixed
 719 sensor nodes. During the field-test 14 bats were equipped with mobile sensor nodes. For the system
 720 performance verification a reference path with 4912 waypoints is used. The reference path itself was
 721 measured by laser equipment during the daytime. In Figure 24 a sensor network with 17 fixed sensor
 722 nodes is shown. The red trajectory represents the ground truth x_k of the reference path. The green

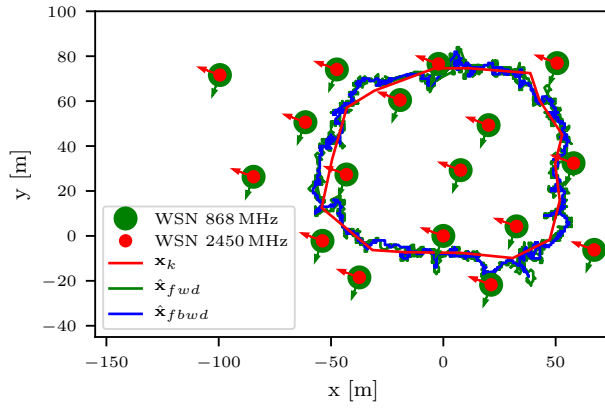


Figure 24. Localization sensor network with 17 nodes, operation at 868 MHz and 2.4 GHz. The ground true path \mathbf{x}_k , the localized filtered path $\hat{\mathbf{x}}_{fwd}$ and localized smoothed path $\hat{\mathbf{x}}_{fbwd}$ is shown.

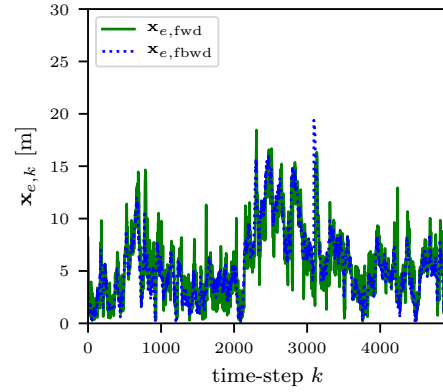


Figure 25. Localization error for all k time-steps of the filtered and smoothed estimated trajectory for the combination of the two frequencies 868 MHz and 2.4 GHz.

Table 1. Average localization error \bar{x}_e of the ML, filtered and smoothed estimated trajectory for the separate frequencies and the combined results.

method	f [MHz]	$\bar{x}_{e,ML}$ [m]	$\bar{x}_{e,fwd}$ [m]	$\bar{x}_{e,fbwd}$ [m]
Δ RSSI	868	36.33	7.72	7.02
Δ RSSI	2450	14.64	6.42	6.28
Δ RSSI	868, 2450	12.93	5.58	5.47

723 and blue trajectory shows the filtered $\hat{\mathbf{x}}_{fwd}$ and smoothed $\hat{\mathbf{x}}_{fbwd}$ localized trajectory by the grid based
 724 particle filter presented in [56] for both frequencies. The localization error $\mathbf{x}_{e,k}$ is calculated with

$$\mathbf{x}_{e,k} = \hat{\mathbf{x}}_k - \mathbf{x}_k. \quad (8)$$

725 where $\hat{\mathbf{x}}_k$ represents the estimated position at the time-step k . The average localization error is
 726 calculated by the mean Euclidean distance with

$$\bar{x}_e = \frac{1}{K} \sum_{k=0}^{K-1} \|\mathbf{x}_{e,k}\|_2 \quad (9)$$

727 where $\|\cdot\|_2$ represents the Euclidean norm. In table 1 the average localization error $\bar{x}_{e,k}$
 728 for the different frequencies 868 MHz and 2.4 GHz is shown. Furthermore the average localization error
 729 for the ML $\bar{x}_{e,ML}$ filtered $\bar{x}_{e,fwd}$ and smoothed $\bar{x}_{e,fbwd}$ localization is shown. The diversity of the
 730 two frequencies lowers the localization error significant. It also shows that a adaptive localization
 731 performance can be achieved by using only one frequency if a lower accuracy is acceptable. By adding
 732 the second frequency a more accurate localization is possible by the drawback of a higher energy
 733 consumption at the mobile node. For further energy saving the transmit rate can be adapted from 1 Hz
 734 to 8 Hz.

735 4.3. Long Range Telemetry

736 The long range functionality as presented in section 3.4 was validated during the Berlin field
 737 test in 2017. For this purpose, a total number of 32 individual bats were equipped with sensor
 738 nodes. A wake-up signal was issued every 2 s for encounter detection and telemetry transmission,
 739 utilizing the combined modulation as described before. Two long range base stations were supplied
 740 on exposed sites around the bats habitat at the forest of *Treptower Park, Planter Wald* and *Konigsheide*.

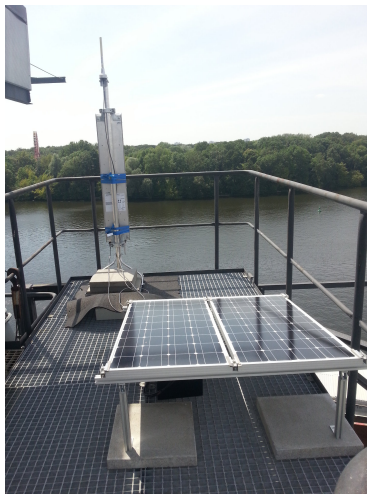


Figure 26. Long range telemetry base station.

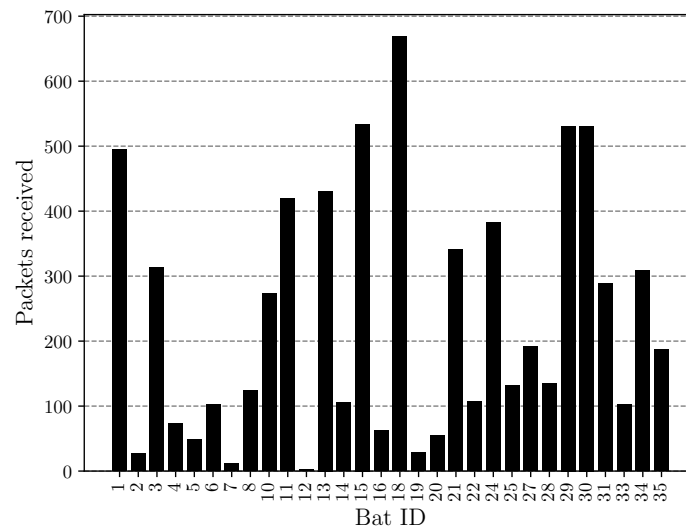


Figure 27. Received long range packets.

741 Figure 26 shows a picture of one of the stations, with its directional antenna facing towards the forest,
 742 the omni-directional antenna on the top and the solar panel for autonomous operation (compare
 743 Section 3.4.2).

744 The field trial was carried out for two weeks. During this time, it was possible to receive over
 745 7.000 complete long range telemetry packets, accounting for over 168.000 bursts in total. Figure 27
 746 shows the total number of received long range data packets in dependence of the bat identification
 747 number. As can be observed, we were able to receive packets from almost every captured bat. The
 748 base stations were located in distances of about 4 km around the forest, in heights comparable to
 749 those applied for the simulations performed in [43,44]. The successful receiving and decoding of
 750 data over this distance shows, that the system layout complies with our simulations on expected
 751 path loss, channel steadiness and rate. Based on those findings, the implementations also proved
 752 their functionality. For the measurements, the bat nodes transmitted a time stamp indicating their
 753 operation time as payload for the long range telemetry, as other data (see section 3.4) was planned,
 754 but the sensors have not been equipped at that time. For the longest operation time, we encountered
 755 a value of 320 h of bat with ID 15, obtained by the very last contact to one of the long range base
 756 stations. When compared to the ground network in Figure 23 with 383 h of operation for ID 15, the
 757 long range transmission deems to deliver reasonable results, being a worthwhile extension to not only
 758 observe bats resting under the trees near the ground network, but also bats flying up in the air while
 759 hunting and outside the tracking range. Summarizing, we showed that we were able to assure a robust
 760 transmission even under the harsh constraints of a limited transmit power of just about 9 dBm, strong
 761 path loss and shadowing of over 150 dB as well as unfavorable antenna alignment of the small bat
 762 node rod antenna relative to our receiving antennas. The measurements substantiated the simulation
 763 results and practical implementations.

764 5. Discussion

765 The BATS system for the first time combines two key features of animal logging, i.e. proximity
 766 sensing among animals and tracking of animals. Proximity information is processed and stored on
 767 the mobile nodes and transferred to ground stations upon contact. Tracking is aimed to achieve high
 768 spatial resolution at the cost of covering relatively small areas of usually a few hectares. Nevertheless,
 769 the overall aim is minimizing the weight of mobile nodes while still achieve a long runtime. Weight

770 is the key parameter for the applicability of a technical animal logging system since low weight
 771 allows tagging of smaller animals. Minimizing weight comes at the cost of reduced runtime and/or
 772 functionality. Therefore, during system development we always aimed to allow flexibility in hardware
 773 (e.g. battery size, number of sensors on a mobile mode) and software settings in order to allow
 774 adaptations of the BATS system to specific applications.

775 A direct comparison of individual parts of the BATS project to other systems is difficult for
 776 multiple reasons. Each part of the project is highly optimized to perform in perfect harmony with the
 777 other components. This way the full performance of each sub-project only takes effect when embedded
 778 in the whole system. This is particularly the case because the ultra low power goal of the overall
 779 system poses strong limitation in system design. This makes the sub-projects not directly comparable
 780 to other system that have full control over the whole experimental setup. Detailed literature about
 781 the performance of individual components of other tracking systems, such as those mentioned in the
 782 related work section (2), is rare. Therefore, only the performance of the system as a whole can be
 783 compared. The table 2 gives an overview about selected related system and compares key parameters
 784 of the systems with each other. Afterwards the systems are compared in more detail.

Table 2. Comparison of related bat tracking systems

system	weight	runtime	spatial resolution	coverage	proximity detection
ATLAS [12]	1.5 g	10 days	5 m	several km ²	no
MOTUS [13]	0.2 to 2.6 g	10 days to 3 years	500 m to 15 km	multiple thousand km ²	no
Biotrack PinPoint 10 [57] (GPS Tracker)	1 g	up to 130 fixes	few meters (GPS)	global	no
ICARUS [16]	5 g	theoretically unlimited because of solar panels	few meters (GPS)	global	no
Encounternet [14]	1.3 g (10 g)	21 hours (2 month)	presence detection	N/A	yes
BATS (this work)	1.0 g (1.3 g)	8 days (17 days)	4 m	several hectares	yes (around 5 m)

785 For encounter detection the Encounternet project (see chapter 2) has similar goals. However, as
 786 seen in Figure 23 the mobile node runtime of the nodes developed in the BATS project is surpassing
 787 the Encounternet node runtime of 21 hours (7.5 days in transmit only mode making them visible for
 788 other nodes/base stations but they can't record meetings themselves) while having the same weight of
 789 around 1.3 g. The BATS system achieves up to 420 hours in full duplex encounter detection. This is
 790 mostly possible because of the wake up receiver based approach of the BATS project. This way the main
 791 receiver and the whole circuit can stay in a low power state most of the time. Other factors benefiting
 792 the long runtime of the BATS sensor nodes is a smart software scheduling and the selection of energy
 793 efficient components even if this means a slightly degraded performance. Other than Encounternet the
 794 BATS project also allows precise location tracking in a predefined ground node network.

795 The tracking part of the BATS system can best be compared to ATLAS, MOTUS and ICARUS as
 796 described in chapter 2. However these systems and the BATS project serve different purpose in animal
 797 research. While the former are focusing on the large scale tracking to for example research migration
 798 patterns, BATS focuses tracking bats with high spatial resolution in a small area of a few hectares.

799 Regarding spatial resolution the ATLAS system and GPS based systems like ICARUS can be
 800 compared to BATS as long as the tracking is performed under ideal conditions. However, based
 801 on the system architecture the ATLAS system reacts sensitive to multipath propagation which has
 802 a negative effect on the precision of the localization. In section 3.3.2 we described how the BATS
 803 system reduces such negative impact due to a new multipath robust design. This allows precise
 804 localization results even in multipath propagation affected areas like forests. While the performance of
 805 GPS based systems can be seen as relatively precise in open areas the precision is reduced in areas
 806 with diminished reception such as vegetated areas. Especially light low power GPS sensortags may
 807 suffer a drop in performance under such conditions. Since in the BATS system the ground stations are
 808 deployed directly in the area which is most relevant to the research, the base station grid can be planed
 809 in a way that coverage is optimized in this area of interest. However, this of course limits the size of
 810 the covered area while GPS can be used global and without ground infrastructure.

811 Especially ATLAS and MOTUS make use of relatively simple sensor nodes with the data
812 processing mostly on the ground stations. Their energy efficiency isn't that critical anymore. This
813 results in relatively long mobile node runtime due to its simplicity. In ICARUS the localization is
814 performed via GPS fixes on the node. Increasing the energy demand drastically but also makes the
815 sensor nodes independent of a ground station network. ICARUS uses mobile nodes with attached
816 solar panels. This way a long runtime can be achieved despite the relatively high current consumption
817 of GPS trackers. This approach can not be applied in the BATS projects since the investigated animals,
818 bats, are nocturnal species and hide in dark roost during day. Still, the theoretically unlimited runtime
819 of the ICARUS nodes is a desirable characteristic of the node. Further research is required to design
820 an energy harvesting system to support the BATS mobile node while taking the strict weight limit as
821 well as the fact that bats are nocturnal animals into account.

822 Similar to ATLAS and MOTUS the BATS project offloads energy-intensive localization to the
823 less energy-constrained ground station network but keeps the mobile nodes highly functional. The
824 localization of an animal is approximated according to the recording of mobile node beacons received
825 by ground nodes that are processed by a central computer providing almost real time information
826 of an animal's location. However, due to the capabilities of the mobile node we can limit sending
827 location beacons only to the area where mobile base stations are in range. This way the overall energy
828 consumption can be reduced especially for individuals spending only short periods of time in the
829 tracking grid.

830 The combination of encounter detection and ground system based localization drastically reduces
831 the amount of so called "blind spots" where no information on the animal can be obtained. GPS based
832 systems for example may have problems getting GPS fixes that determine the current location in thick
833 forest environments and places like roosts or caves. In unknown locations the BATS system still allows
834 indirectly monitoring the animals' behavior by collecting encounter data among tagged animals or - if
835 such locations are known - fixed sensor nodes may be installed in these places that act as normal bat
836 nodes. This way fixed nodes record encounter data and report on the identity of individual tagged
837 bats in range. In such scenarios we can precisely assess, e.g., the time an individual left the roost for
838 hunting.

839 Other than all mentioned systems the BATS system implements a quasi energy neutral long range
840 telemetry system that allows receiving data even if the bat leaves the area of high interest where
841 a the precise tracking and/or data download takes place. Thanks to embedding the long range
842 telemetry signal in the beacons sent out for encounter detection and making use of a newly developed
843 transmission scheme (as described in section 3.4.1) the long range telemetry is included at practically
844 no extra current consumption on the mobile node. We achieve a high energy efficiency and still can
845 receive the signal up to 4 km away from the long range antennas despite high path loss, shadowing
846 and generally highly varying channel due to the bats movement speed.

847 Being able to adapt its behavior based on the current situation to increase energy-efficiency while
848 maintaining full functionality when needed is the key feature of the BATS system. Various functions on
849 the mobile node are automatically regulated upon demand by switching between different operation
850 levels including a sleep mode. Such adaptive functionality is achieved by introducing so-called zones
851 which are set by receiving beacons from ground stations. Similar to only send localization beacons at
852 high frequency while being in the tracking grid and not sending them while being outside the grid
853 to save energy, for encounter logging the beaconing frequency is reduced as soon as the animal is
854 within the roost. Here the environment is rather stable thus the time between encounter beacons is
855 much longer. Following this zone principle certain functionalities can be enabled respectively disabled
856 and parameters of the tags can be changed depending on the current application of the system. This
857 functionality enables the BATS system to track bats inside the tracking grid at high spatial and temporal
858 resolution while no localization beacons are sent at all when bats are outside the tracking grid to save
859 energy. Comparable systems either transmit beacons continuously or schedule the sending based on
860 programmed time slots regardless of the location of the animal. Apart from external control of the

861 nodes behavior with beacons the mobile node can schedule the use of on board peripheral resources,
862 like the NVRAM storage, itself. This allows the system to keep components turned off for the majority
863 of the time and only power them when required.

864 A particularly energy intensive task of the mobile node is the transmission of stored data to the
865 ground station network. Combining multiple packages to bursts allowed the reduction of energy by
866 40% to 30 μ J per packet. Further reductions may be possible by omitting checksums in the transmitted
867 packages. However, this would lead to an increased packet loss and render the recorded data unusable.

868 Data retrieval from mobile nodes is a crucial step of the BATS system. It occurs upon contact
869 of mobile nodes to ground stations at a distance of up to approximately 150 m depending on the
870 environment. Much longer data retrieval distances of up to 4 km were achieved by the implementation
871 of long-range telemetry (see chapter 3.4).

872 Technical development of the BATS system was subjected to multiple iterations for optimization
873 and addition of new features. An overview about a previous version can be found in [58]. Meanwhile,
874 it is possible to track 60 animals at the same time instead to 28 previously. The spatial precision of the
875 flight trajectory was substantially improved from 7 m average error to 4 m. In addition, the current
876 mobile node is characterized by lighter hardware and slimmer dimensions due to improved hardware
877 components and a redesign of the board outlay. Low energy-consumption was an important criterion
878 in selecting among commercially available components for the mobile nodes. Thanks to the now
879 available on board NVRAM the system also allows recording of larger data sets (e.g. more encounters)
880 until download upon contact to a ground station. The lower weight of the node without battery and
881 lower power consumption allows the use of batteries with higher capacity and generally results into
882 an extended runtime.

883 6. Conclusion and Future Work

884 The wide range of available technical systems for animal logging can largely differ in their
885 technical features determining their applicability studying animals in their natural habitat 2. The BATS
886 system meets simultaneously the needs for proximity sensing and local high-resolution tracking in a
887 single system by optimizing energy use. This unique combination allows a wide range of applications
888 in the fields of sociobiology, behavioral ecology, movement ecology or physiological ecology. The
889 small size and weight of the mobile nodes and the flexibility of the whole system allow investigating a
890 broad spectrum of species.

891 Depending on the actual use case individual functionalities of the system can be disabled to
892 provide a longer runtime and certain functions can flexibly be enabled/disabled in the field based on
893 the current location/situation of the tag. The adaptive approach of the BATS system leads to high
894 quality data when required while at the same time maintaining an overall long runtime.

895 The current system is actively used in biological studies [59,60] and creates rich data sets on the
896 studied animals.

897 The applicability of the BATS system can be expanded by adding new sensors like an accelerometer
898 or magnetometer. Thus, it represents a new modular system that can be redesigned according to the
899 needs for a specific application. Both, hardware and software adjustments are important measures
900 to reach the minimal weight limits of mobile nodes, which strongly determines the range of animal
901 species that can be studied.

902 Still, even the current version can be used for multiple further biological studies regarding (social)
903 behavior in bats and similar sized (airborne) animals. The paper has shown, that for studies that rely
904 on encounter data either with or without localization the BATS system has outstanding performance
905 and is capable of generating precise results.

906 **Author Contributions:** “This work is giving an overview about the BATS Research Group’s work. The chapter 3
907 is split in the corresponding sub-groups of whom each wrote their section. Section 3.1: Writing: N.D.; Supervision,
908 Funding: A.K.; Section 3.2: Writing: B.C., P.W.; Supervision, Funding: R.K. W.SP.; Section 3.3: Writing: M.H.,
909 T.N.; Supervision, Funding: J.T.; Section 3.4: Writing: M.S.; Supervision, Funding: J.R.; Section 3.5: Writing: S.H.;

910 Supervision, Funding: K.M.W.; Section 3.6: Writing: M.N.; Supervision, Funding: F.D.; Section 4: Writing: N.D.,
 911 M.H., T.N., M.S.; Other chapters: Writing: N.D.; Biologic Aspects in all Chapters: Writing: S.R.; Supervision,
 912 Funding: F.M.; Project Administration, R.W.;

913 **Funding:** This work is funded by German Science Foundation DFG grant FOR 1508, Research Unit BATS
 914 "Dynamic Adaptable Applications for Bat Tracking by Embedded Communicating Systems".

915 **Conflicts of Interest:** The authors declare no conflict of interest. The founding sponsors had no role in the design
 916 of the study; in the collection, analyses, or interpretation of data; in the writing of the manuscript, and in the
 917 decision to publish the results.

918

- 919 1. Wilmers, C.C.; Nickel, B.; Bryce, C.M.; Smith, J.A.; Wheat, R.E.; Yovovich, V. The golden age of bio-logging:
 920 how animal-borne sensors are advancing the frontiers of ecology. *Ecology* **2015**, *96*, 1741–1753.
- 921 2. Kays, R.; Crofoot, M.C.; Jetz, W.; Wikelski, M. Terrestrial animal tracking as an eye on life and planet.
 922 *Science* **2015**, *348*, aaa2478.
- 923 3. Krause, J.; Krause, S.; Arlinghaus, R.; Psorakis, I.; Roberts, S.; Rutz, C. Reality mining of animal social
 924 systems. *Trends in ecology & evolution* **2013**, *28*, 541–551.
- 925 4. Tucker, M.A.; Böhning-Gaese, K.; Fagan, W.F.; Fryxell, J.M.; Van Moorter, B.; Alberts, S.C.; Ali, A.H.;
 926 Allen, A.M.; Attias, N.; Avgar, T.; others. Moving in the Anthropocene: Global reductions in terrestrial
 927 mammalian movements. *Science* **2018**, *359*, 466–469.
- 928 5. Strandburg-Peshkin, A.; Farine, D.R.; Couzin, I.D.; Crofoot, M.C. Shared decision-making drives collective
 929 movement in wild baboons. *Science* **2015**, *348*, 1358–1361.
- 930 6. Silva, R.; Afán, I.; Gil, J.A.; Bustamante, J. Seasonal and circadian biases in bird tracking with solar GPS-tags.
 931 *PLOS ONE* **2017**, *12*, 1–19. doi:10.1371/journal.pone.0185344.
- 932 7. Bodey, T.W.; Cleasby, I.R.; Bell, F.; Parr, N.; Schultz, A.; Votier, S.C.; Bearhop, S. A phylogenetically
 933 controlled meta-analysis of biologging device effects on birds: Deleterious effects and a call for more
 934 standardized reporting of study data. *Methods in Ecology and Evolution* **2018**, *9*, 946–955.
- 935 8. Vandenabeele, S.P.; Shepard, E.L.; Grogan, A.; Wilson, R.P. When three per cent may not be three per cent;
 936 device-equipped seabirds experience variable flight constraints. *Marine Biology* **2012**, *159*, 1–14.
- 937 9. Barron, D.G.; Brawn, J.D.; Weatherhead, P.J. Meta-analysis of transmitter effects on avian behaviour and
 938 ecology. *Methods in Ecology and Evolution* **2010**, *1*, 180–187.
- 939 10. Amelon, S.K.; Dalton, D.C.; Millspaugh, J.J.; Wolf, S.A. Radiotelemetry; techniques and analysis. In: Kunz,
 940 Thomas H.; Parsons, Stuart, eds. *Ecological and behavioral methods for the study of bats*. Baltimore: Johns Hopkins
 941 University Press: 57-77. **2009**, pp. 57–77.
- 942 11. O'Mara, M.T.; Wikelski, M.; Dechmann, D.K. 50 years of bat tracking: device attachment and future
 943 directions. *Methods in Ecology and Evolution* **2014**, *5*, 311–319.
- 944 12. Weiser, A.W.; Orchan, Y.; Nathan, R.; Charter, M.; Weiss, A.J.; Toledo, S. Characterizing the
 945 Accuracy of a Self-Synchronized Reverse-GPS Wildlife Localization System. 2016 15th ACM/IEEE
 946 International Conference on Information Processing in Sensor Networks (IPSN), 2016, pp. 1–12.
 947 doi:10.1109/IPSN.2016.7460662.
- 948 13. Taylor, P.; Crewe, T.; Mackenzie, S.; Lepage, D.; Aubry, Y.; Crysler, Z.; Finney, G.; Francis, C.; Guglielmo, C.;
 949 Hamilton, D.; others. The Motus Wildlife Tracking System: a collaborative research network to enhance
 950 the understanding of wildlife movement. *Avian Conservation and Ecology* **2017**, *12*.
- 951 14. Levin, I.I.; Zonana, D.M.; Burt, J.M.; Safran, R.J. Performance of Encournternet Tags: Field Tests of
 952 Miniaturized Proximity Loggers for Use on Small Birds. *PLoS One* **2015**.
- 953 15. Rutz, C.; Burns, Z.T.; James, R.; Ismar, S.M.; Burt, J.; Otis, B.; Bowen, J.; Clair, J.J.S.
 954 Automated mapping of social networks in wild birds. *Current Biology* **2012**, *22*, R669 – R671.
 955 doi:https://doi.org/10.1016/j.cub.2012.06.037.
- 956 16. Wikelski, M.; Rienks, F. The ICARUS White Paper. Technical report, Max Planck Institute for Ornithology,
 957 2008.
- 958 17. Collotta, M.; Pau, G.; Talty, T.; Tonguz, O.K. Bluetooth 5: A Concrete Step Forward toward the IoT. *IEEE*
 959 *Communications Magazine* **2018**, *56*, 125–131. doi:10.1109/MCOM.2018.1700053.
- 960 18. Pau, G.; Collotta, M.; Maniscalco, V. Bluetooth 5 Energy Management through a Fuzzy-PSO Solution for
 961 Mobile Devices of Internet of Things. *energies*, 2017, Vol. 10. doi:10.3390/en10070992.

- 962 19. Duda, N.; Weigel, R.; Koelpin, A. Enhanced mobile node design for small size animal borne wireless sensor
963 nodes with encounter detection and localization. 2018 11th German Microwave Conference (GeMiC), 2018,
964 pp. 123–126. doi:10.23919/GEMIC.2018.8335044.
- 965 20. Kunz, Thomas H Parsons, S., Ecological and behavioral methods for the study of bats; Johns Hopkins
966 University Press, 2009; chapter Radiotelemetry: Techniques and analysis., pp. 57–77.
- 967 21. Wägemann, P.; Distler, T.; Hönig, T.; Janker, H.; Kapitza, R.; Schröder-Preikschat, W. Worst-Case Energy
968 Consumption Analysis for Energy-Constrained Embedded Systems. Proceedings of the 27th Euromicro
969 Conference on Real-Time Systems (ECRTS '15), 2015, pp. 105–114.
- 970 22. Wägemann, P.; Dietrich, C.; Distler, T.; Ulbrich, P.; Schröder-Preikschat, W. Whole-System Worst-Case
971 Energy-Consumption Analysis for Energy-Constrained Real-Time Systems. Proceedings of the 30th
972 Euromicro Conference on Real-Time Systems (ECRTS '18), 2018, pp. 24:1–24:25.
- 973 23. Ash, J.; Potter, L. Sensor network localization via received signal strength measurements with directional
974 antennas. Proc. of the 2004 Allerton Conference on Communication, Control, and Computing, 2004, pp.
975 1861–1870.
- 976 24. Nowak, T.; Hartmann, M.; Patino-Studencki, L.; Thielecke, J. Fundamental Limits in RSSI-based
977 direction-of-arrival estimation. 2016 13th Workshop on Positioning, Navigation and Communications
978 (WPNC), 2016, pp. 1–6. doi:10.1109/WPNC.2016.7822837.
- 979 25. Malajner, M.; Planinsic, P.; Gleich, D. Angle of Arrival Estimation Using RSSI and Omnidirectional
980 Rotatable Antennas. *IEEE Sensors Journal* **2012**, *12*, 1950–1957. doi:10.1109/JSEN.2011.2182046.
- 981 26. Malajner, M.; Gleich, D.; Planinšič, P. Angle of Arrival Measurement Using Multiple Static Monopole
982 Antennas. *IEEE Sensors Journal* **2015**, *15*, 3328–3337. doi:10.1109/JSEN.2014.2386537.
- 983 27. Hood, B.N.; Barooah, P. Estimating DoA From Radio-Frequency RSSI Measurements Using an Actuated
984 Reflector. *IEEE Sensors Journal* **2011**, *11*, 413–417. doi:10.1109/JSEN.2010.2070872.
- 985 28. Cidronali, A.; Maddio, S.; Giorgetti, G.; Manes, G. Analysis and Performance of a Smart Antenna for
986 2.45-GHz Single-Anchor Indoor Positioning. *IEEE Transactions on Microwave Theory and Techniques* **2010**,
987 *58*, 21–31. doi:10.1109/TMTT.2009.2035947.
- 988 29. Kamarudin, M.R.; Nechayev, Y.I.; Hall, P.S. Onbody Diversity and Angle-of-Arrival Measurement
989 Using a Pattern Switching Antenna. *IEEE Transactions on Antennas and Propagation* **2009**, *57*, 964–971.
990 doi:10.1109/TAP.2009.2014597.
- 991 30. Kulas, L. Simple 2-D Direction-of-Arrival Estimation Using an ESPAR Antenna. *IEEE Antennas and Wireless*
992 *Propagation Letters* **2017**, *16*, 2513–2516. doi:10.1109/LAWP.2017.2728322.
- 993 31. Pohlmann, R.; Zhang, S.; Jost, T.; Dammann, A. Power-based direction-of-arrival estimation using a single
994 multi-mode antenna. 2017 14th Workshop on Positioning, Navigation and Communications (WPNC),
995 2017, pp. 1–6. doi:10.1109/WPNC.2017.8250056.
- 996 32. Passafiume, M.; Maddio, S.; Cidronali, A.; Manes, G. MUSIC algorithm for RSSI-based DoA estimation on
997 standard IEEE 802.11/802.15. x systems. *World Sci. Eng. Acad. Soc. Trans. Signal Process* **2015**, *11*, 58–68.
- 998 33. Hartmann, M.; Nowak, T.; Patino-Studencki, L.; Robert, J.; Heuberger, A.; Thielecke, J. A Low-Cost
999 RSSI-Based Localization System for Wildlife Tracking. *IOP Conference Series: Materials Science and*
1000 *Engineering* **2016**, *120*, 012004. doi:10.1088/1757-899X/120/1/012004.
- 1001 34. Balanis, C.A. *Modern Antenna Handbook*; Wiley-Interscience: New York, NY, USA, 2008.
- 1002 35. Nowak, T.; Hartmann, M.; Thielecke, J. Unified performance measures in network localization. *EURASIP*
1003 *Journal on Advances in Signal Processing* **2018**, *2018*, 48. doi:10.1186/s13634-018-0570-8.
- 1004 36. Yang, Y.; Blum, R.S. MIMO radar waveform design based on mutual information and minimum
1005 mean-square error estimation. *IEEE Transactions on Aerospace and Electronic Systems* **2007**, *43*, 330–343.
1006 doi:10.1109/TAES.2007.357137.
- 1007 37. Chen, Y.; Goldsmith, A.J.; Eldar, Y.C. On the Minimax Capacity Loss Under Sub-Nyquist Universal
1008 Sampling. *IEEE Transactions on Information Theory* **2017**, *63*, 3348–3367. doi:10.1109/TIT.2017.2695541.
- 1009 38. Kipnis, A.; Goldsmith, A.J.; Eldar, Y.C. Sub-Nyquist sampling achieves optimal rate-distortion. 2015 IEEE
1010 Information Theory Workshop (ITW), 2015, pp. 1–5. doi:10.1109/ITW.2015.7133113.
- 1011 39. Kipnis, A.; Reeves, G.; Eldar, Y.C.; Goldsmith, A.J. Fundamental limits of compressed sensing under
1012 optimal quantization. Information Theory (ISIT), 2017 IEEE International Symposium on, 2017.

- 1013 40. Gu, Y.; Goodman, N.A. Information-Theoretic Compressive Sensing Kernel Optimization and Bayesian
1014 Cramer Rao Bound for Time Delay Estimation. *IEEE Transactions on Signal Processing* **2017**, *65*, 4525–4537.
1015 doi:10.1109/TSP.2017.2706187.
- 1016 41. Nowak, T.; Hartmann, M.; Tröger, H.M.; Patino-Studencki, L.; Thielecke, J. Probabilistic multipath
1017 mitigation in RSSI-based direction-of-arrival estimation. 2017 IEEE International Conference on
1018 Communications Workshops (ICC Workshops), 2017, pp. 1024–1029. doi:10.1109/ICCW.2017.7962793.
- 1019 42. Proakis, J. *Digital communications*; McGraw-Hill: Boston, 2008.
- 1020 43. Schadhauer, M.; Robert, J.; Heuberger, A. Concept for an Adaptive Low Power Wide Area (LPWA) Bat
1021 Communication Network. Smart SysTech 2016; European Conference on Smart Objects, Systems and
1022 Technologies, 2016, pp. 1–9.
- 1023 44. Schadhauer, M.; Robert, J.; Heuberger, A. Design of Autonomous Base Stations for Low Power Wide
1024 Area (LPWA) Communication. Smart SysTech 2017; European Conference on Smart Objects, Systems and
1025 Technologies, 2017, pp. 1–8.
- 1026 45. Kilian, G.; Petkov, H.; Psiuk, R.; Lieske, H.; Beer, F.; Robert, J.; Heuberger, A. Improved Coverage for
1027 Low-Power Telemetry Systems using Telegram Splitting. Smart SysTech 2013; European Conference on
1028 Smart Objects, Systems and Technologies, 2013, pp. 1–6.
- 1029 46. Kilian, G.; Breiling, M.; Petkov, H.H.; Lieske, H.; Beer, F.; Robert, J.; Heuberger, A. Increasing Transmission
1030 Reliability for Telemetry Systems Using Telegram Splitting. *IEEE Transactions on Communications* **2015**,
1031 *63*, 949–961. doi:10.1109/TCOMM.2014.2386859.
- 1032 47. Rauh, S.; Robert, J.; Schadhauer, M.; Heuberger, A. LPWAN Occupancy Model Parameter Identification
1033 for License Exempt sub-GHz Frequency Bands. German Microwave Conference (GeMiC), 2018.
- 1034 48. Soller, D.; Jaumann, T.; Kilian, G.; Robert, J.; Heuberger, A. DFC++ Processing Framework Concept:
1035 A Novel Framework Approach for Flexible Signal Processing on Embedded Systems. *Journal of Signal
1036 Processing Systems* **2016**, pp. 1–10. doi:10.1007/s11265-016-1174-x.
- 1037 49. Eng, T.; Kong, N.; Milstein, L.B. Comparison of diversity combining techniques for Rayleigh-fading
1038 channels. *IEEE Transactions on Communications* **1996**, *44*, 1117–1129. doi:10.1109/26.536918.
- 1039 50. Wang, Y.; Noubir, G. Distributed Cooperation and Diversity for Hybrid Wireless Networks. *IEEE
1040 Transactions on Mobile Computing* **2013**, *12*, 596–608. doi:10.1109/TMC.2012.38.
- 1041 51. Mukherjee, S.; Avidor, D. Effect of microdiversity and correlated macrodiversity on outages in a cellular
1042 system. *IEEE Transactions on Wireless Communications* **2003**, *2*, 50–58. doi:10.1109/TWC.2002.806363.
- 1043 52. Sediq, A.B.; Yanikomeroğlu, H. Diversity Combining of Signals with Different Modulation Levels in
1044 Cooperative Relay Networks. 68th IEEE Vehicular Technology Conference (VTC2008-Fall); IEEE: Calgary,
1045 Canada, 2008; pp. 1–5. doi:10.1109/VETEFC.2008.173.
- 1046 53. Nabeel, M.; Bloessl, B.; Dressler, F. Low-Complexity Soft-Bit Diversity Combining for Ultra-Low Power
1047 Wildlife Monitoring. IEEE Wireless Communications and Networking Conference (WCNC 2017); IEEE:
1048 San Francisco, CA, 2017. doi:10.1109/WCNC.2017.7925504.
- 1049 54. Nabeel, M.; Bloessl, B.; Dressler, F. Selective Signal Sample Forwarding for Receive Diversity in
1050 Energy-Constrained Sensor Networks. IEEE International Conference on Communications (ICC 2017);
1051 IEEE: Paris, France, 2017. doi:10.1109/ICC.2017.7996320.
- 1052 55. Nabeel, M.; Bloessl, B.; Dressler, F. Efficient Receive Diversity in Distributed Sensor Networks using
1053 Selective Sample Forwarding. *IEEE Transactions on Green Communications and Networking* **2018**, *2*, 336–345.
1054 doi:10.1109/TGCN.2017.2780196.
- 1055 56. Hartmann, M.; Nowak, T.; Pfadenhauer, O.; Thielecke, J.; Heuberger, A. A Grid-based Filter for Tracking
1056 Bats Applying Field Strength Measurements. Proceedings of the 2016 IEEE/IFIP Wireless On-demand
1057 Network systems and Services Conference, 2016, pp. 184–191.
- 1058 57. Biotrack Ltd. PinPoint 10. <http://www.biotrack.co.uk/pinpoint-gps.php#s4>. Accessed: 2018-09-20.
- 1059 58. Dressler, F.; Ripperger, S.; Hierold, M.; Nowak, T.; Eibel, C.; Cassens, B.; Mayer, F.; Meyer-Wegener, K.;
1060 Koelpin, A. From Radio Telemetry to Ultra-Low Power Sensor Networks - Tracking Bats in the Wild. *IEEE
1061 Communications Magazine* **2016**, *54*, 129–135. doi:10.1109/MCOM.2016.7378438.
- 1062 59. Ripperger, S.; Josic, D.; Hierold, M.; Koelpin, A.; Weigel, R.; Hartmann, M.; Page, R.; Mayer, F. Automated
1063 proximity sensing in small vertebrates: design of miniaturized sensor nodes and first field tests in bats.
1064 *Ecology and evolution* **2016**, *6*, 2179–2189.

1065 60. Ripperger, S.; Guenther, L.; Wieser, H.; Duda, N.; Hierold, M.; Cassens, B.; Kapitza, R.; Koelpin, A.; Mayer,
1066 F. Proximity sensors reveal social information transfer in maternity colonies of Common noctule bats.
1067 *bioRxiv* **2018**. doi:10.1101/421974.

1068 © 2018 by the authors. Submitted to *Sensors* for possible open access publication under the terms and conditions
1069 of the Creative Commons Attribution (CC BY) license (<http://creativecommons.org/licenses/by/4.0/>).